

## The off-shell Veneziano amplitude in Schnabl gauge

LEONARDO RASTELLI

*C.N. Yang Institute for Theoretical Physics  
Stony Brook University  
Stony Brook, NY 11794, USA*

BARTON ZWIEBACH

*Center for Theoretical Physics  
Massachusetts Institute of Technology  
Cambridge, MA 02139, USA*

### Abstract

We give a careful definition of the open string propagator in Schnabl gauge and present its worldsheet interpretation. The propagator requires two Schwinger parameters and contains the BRST operator. It builds surfaces by gluing strips of variable width to the left and to the right of off-shell states with contracted or expanded local frames. We evaluate explicitly the four-point amplitude of off-shell tachyons. The computation involves a subtle boundary term, crucial to enforce the correct exchange symmetries. Interestingly, the familiar on-shell physics emerges even though string diagrams produce Riemann surfaces more than once. Off-shell, the amplitudes do not factorize over intermediate on-shell states.

# Contents

<b>1</b>	<b>Introduction</b>	<b>2</b>
<b>2</b>	<b>The propagator, <math>B/L</math>, and <math>B^*/L^*</math></b>	<b>6</b>
2.1	Deriving the propagator . . . . .	6
2.2	CFT representation of $B/L$ . . . . .	7
2.3	CFT representation of $B^*/L^*$ . . . . .	11
<b>3</b>	<b>The off-shell Veneziano amplitude: first two diagrams</b>	<b>13</b>
3.1	First diagram . . . . .	14
3.2	Second diagram . . . . .	19
<b>4</b>	<b>Boundary term and exchange symmetry</b>	<b>25</b>
4.1	Boundary term . . . . .	27
4.2	Proof of exchange symmetry . . . . .	31
4.3	The propagator revisited . . . . .	36
<b>5</b>	<b>Discussion</b>	<b>38</b>
<b>A</b>	<b>Notation and algebraic identities</b>	<b>40</b>
A.1	Basic properties . . . . .	40
A.2	Reordering formulas . . . . .	41
A.3	Wedge states . . . . .	42
<b>B</b>	<b>Correlators on the cylinder</b>	<b>43</b>
<b>C</b>	<b>Proof of the rearrangement formula</b>	<b>44</b>

## 1 Introduction

Off-shell amplitudes have been the subject of much interest throughout the history of string theory. It was suspected from the beginning that the celebrated Veneziano four-point amplitude [1] for the on-shell scattering of open string tachyons would have a sensible off-shell extension. Even three-point vertices would have off-shell extensions. It was clear that a consistent *set* of off-shell amplitudes would emerge from a field theory of strings.

Although the amplitudes of light-cone string field theory [2] make sense off-shell, their properties are unusual. With the development of a Lorentz covariant open string field theory [3],

the study of off-shell amplitudes began in earnest. These studies had useful applications. In fact, the expected properties of off-shell closed string amplitudes gave constraints [4, 5] that helped in the construction of closed string field theory [6]. Off-shell amplitudes were studied mostly using the Siegel gauge. It was learned that:

1. The amplitudes have permutation symmetry among scattering states.
2. The amplitudes are integrals over sections of fiber bundles with base the moduli spaces of Riemann surfaces and fibers spanning the possible choices of local coordinates at the punctures where the scattering states are inserted. Ignoring coordinates at the punctures, each Riemann surface contributes only once to the amplitude.
3. The amplitudes satisfy *factorization*: near poles, all of which must arise from the propagator, the amplitude is a product of the relevant off-shell vertices.

The first property arises because the vertices in the string field theory action are symmetric and so is the propagator.<sup>1</sup> The second property implies that the string diagrams for a given amplitude give a construction of the appropriate moduli space of Riemann surfaces: they produce all surfaces of fixed genus and fixed number of punctures, each surfaced produced only once. The third property arises because string diagrams at factorization develop infinitely long strips (or tubes, in closed string theory) that if cut, result in two allowed subdiagrams<sup>2</sup> which provide the two off-shell factors.

Siegel gauge provides amplitudes that obey the above properties, but not all gauges do. Off-shell light-cone amplitudes do not satisfy property 1 because the string diagrams break the symmetry among states by assigning to them values of the light-cone momentum  $p^+$  all of which cannot be the same. They do not satisfy property 3 either, because the Schwinger parameters associated with propagators are sometimes not independent.

In this paper we begin a detailed study of off-shell amplitudes in Schnabl gauge, the gauge in which it was possible to obtain an analytic form for the tachyon vacuum string field [7]. The string field that represents a finite marginal deformation by a regular marginal operator is another solution in Schnabl gauge [8, 9]. Other analytic solutions [10, 11, 12, 13] use the wedge states [14, 15, 16, 17, 18] that are natural in Schnabl gauge, but do not actually satisfy the gauge condition. Recent related work appears in [19]–[28].

---

<sup>1</sup>In open string field theory the vertices are only cyclically symmetric, full symmetry arises by summing over inequivalent orderings. In closed string field theory the vertices are, by construction, fully symmetric.

<sup>2</sup>There are also factorizations in which cutting a line does not split the diagram into two separate pieces.

The simplest amplitude to consider is the Veneziano amplitude. Its off-shell version in Schnabl gauge is the central topic in this paper. In Siegel gauge the Veneziano amplitude was first discussed by Giddings [29], who found the conformal map from the string diagram to the upper-half plane and then showed that the amplitude would reproduce the familiar on-shell result. The closed-form expression for the amplitude is fairly complicated as it requires constraints that involve elliptic functions and their inverses. Further analysis and applications were discussed in [30, 31].

The off-shell Veneziano amplitude in Schnabl gauge was first examined in the useful paper by Fuji, Nakayama, and Suzuki [32], who used an algebraic approach. We use the more geometrical conformal field theory interpretation of the amplitude and emphasize at each step the integrations over the moduli of the relevant Riemann surfaces. As it turns out, we have found that a subtle boundary term is missing<sup>3</sup> in the computation of [32]. This term is needed because the naive computation gives a result that violates the manifest exchange symmetry between incoming and outgoing states of the string amplitude.

As first stated in [7], and as we review in §2, a propagator  $\mathcal{P}$  that *formally* inverts the BRST operator in the gauge  $B\Psi = 0$  is

$$\mathcal{P} \equiv \frac{B}{L} Q \frac{B^*}{L^*}. \quad (1.1)$$

Here  $\star$  denotes BPZ conjugation,  $Q$  is the BRST operator, and  $B$  and  $L$  denote, respectively, the antighost and the Virasoro zero modes in the sliver frame.<sup>4</sup> In Siegel gauge each propagator  $b_0/L_0$  uses one Schwinger parameter, exactly the number needed to produce the moduli space of surfaces with punctures on the boundary. In Schnabl gauge the propagator uses two Schwinger parameters, one to represent  $1/L$  and another to represent  $1/L^*$ . With two parameters for each internal line we overcount moduli space and each surface is produced an infinite number of times. We exhibit this phenomenon explicitly for the off-shell Veneziano amplitude. It is the presence of  $Q$  that makes this overcounting compatible with the familiar on-shell result.

In computations one may use  $\{Q, B^*\} = L^*$  and naively assume that this  $L^*$  cancels with the  $1/L^*$  in  $\mathcal{P}$  to give

$$\mathcal{P} \stackrel{?}{=} \frac{B}{L} - \frac{B B^*}{L L^*} Q. \quad (1.2)$$

This is the propagator used in [32] to compute the Veneziano amplitude<sup>5</sup>. By looking at the factorization properties of the  $s$ -channel contribution to the off-shell four-point amplitude following from (1.2) we find that the exchange symmetry under  $(p_1, p_2) \leftrightarrow (p_3, p_4)$  is violated. We then demonstrate that the requisite symmetry is restored if we include on the right-hand

---

<sup>3</sup>There are some further small disagreements in our computations.

<sup>4</sup>Our conventions are the same as in [14, 23, 9] and are reviewed in appendix A.

<sup>5</sup>The presentation of B. Zwiebach in Strings 2007 (Madrid) also used this propagator.

side of (1.2) an extra boundary term that arises when  $1/L^*$  is represented by a Schwinger parameter with a cutoff  $\Lambda^*$ :

$$- \lim_{\Lambda^* \rightarrow \infty} \frac{1}{2} \frac{B}{L} e^{-\Lambda^* L^*}. \quad (1.3)$$

We explain how this term arises from a regulated version of (1.1) where the Schwinger representation of the propagator uses two independent cutoffs  $\Lambda$  and  $\Lambda^*$  and a symmetric limit is used to take them to infinity. We check that this concrete definition for the propagator provides an inverse for the BRST operator. Further analysis shows that the boundary term that arises from (1.3) is actually antisymmetric under the exchange. Hence a symmetrized version of the propagator (where  $Q$  is moved both to the left and to the right) requires no boundary terms. We conclude that, after proper care of all subtleties, property 1 holds.

Property 2 does not hold. In Schnabl gauge off-shell amplitudes include finite integrals over parameters that *do not* change the moduli; the string diagrams produce Riemann surfaces more than once. This is illustrated in the Veneziano amplitude, where we find a coordinate for the redundant direction of integration that simplifies the amplitude considerably. The possible existence of a set of consistent off-shell amplitudes that are not built by integration over moduli space is probably the most novel and nontrivial feature of the Schnabl gauge.

We were somewhat surprised that property 3 does not hold – the off-shell Veneziano amplitude does not exhibit factorization. This is checked, at lowest level, by looking at the pole that arises when the intermediate line is an on-shell tachyon. We find that the residue is *not* the product of two Witten vertices with two lines off-shell and one line on-shell. It is, instead, the symmetrized product of two different vertices. Of course, the string diagrams do not suggest off-shell factorization since there is no long strip separating identical looking vertices.

This paper begins in §2 with an explanation for (1.1). We then discuss the CFT interpretation of  $B/L$  acting on star products of off-shell states. Our result here is a generalization of the on-shell result in [9]. We find a related CFT interpretation for the action of  $B^*/L^*$ . These formulas are the analogs of the simple strip-plus-antighost representation of the Siegel gauge propagator  $b_0/L_0$ . In §3 we compute the two diagrams that correspond (1.2). We rewrite the amplitudes in terms of moduli in order to simplify the results. As would be expected, the formulas are much simpler to write and evaluate than the corresponding ones in Siegel gauge. By examination of the factorization on on-shell tachyons, we note that the amplitude computed so far fails to have the expected symmetry under the exchange  $(p_1, p_2) \leftrightarrow (p_3, p_4)$ . In §4 we identify the culprit in a subtle boundary term that happens not to vanish. We explain how the boundary term arises from a suitably regulated propagator and demonstrate that its addition restores the exchange symmetry. We revisit the formal arguments of §2.1 and show that with

this prescription the propagator provides an inverse for the BRST operator. The final formulae for the off-shell Veneziano amplitude are given in (4.51) and (4.54). In §5 we discuss our results and some interesting open questions. A collection of useful formulas have been relegated to three appendices.

## 2 The propagator, $B/L$ , and $B^*/L^*$

### 2.1 Deriving the propagator

An open string field  $\Psi$  is in Schnabl gauge if it satisfies

$$B\Psi = 0. \quad (2.1)$$

Here  $B$  denotes the antighost zero mode in the conformal frame of the sliver and is a linear combination of  $b_{2n}$  oscillators,  $n \geq 0$ . The operator  $B$  is not BPZ even,  $B^* \neq B$ . Clearly, the operator  $B$  squares to zero,  $B^2 = 0$ . The full state space  $\mathcal{H}$  breaks into two complementary vector subspaces  $S$  and  $S'$ , where  $S$  is the subspace of states that satisfy the gauge condition (2.1). To show this consider an operator  $C$  such that  $C^2 = 0$  and  $\{B, C\} = 1$ . The form of  $C$  is not relevant, but one could take  $C = c_0$ , for example. While  $c_0^* = -c_0$ , in general  $C^* \neq -C$ . From BPZ conjugation rules it follows that  $\{B^*, C^*\} = -1$ . Then introduce the orthogonal projectors

$$P = BC, \quad P' = CB. \quad (2.2)$$

Indeed, one readily verifies that  $P^2 = P$ ,  $P'^2 = P'$ ,  $PP' = P'P = 0$ , and  $P + P' = 1$ . We have  $P : \mathcal{H} \rightarrow S$  because  $BP = 0$ . We also note that

$$P^* = -C^*B^*. \quad (2.3)$$

In Siegel gauge ( $b_0\Psi = 0$ ) one has  $P = b_0c_0$ ,  $P' = c_0b_0$ , and  $P^* = -c_0^*b_0^* = c_0b_0 = P'$ . In Schnabl gauge,  $P^* \neq P'$ .

To find the propagator one considers the kinetic operator  $\mathcal{K}$  obtained by restricting the kinetic term to string fields in the gauge slice, *i.e.* string fields of the form  $P\Psi$ :

$$\frac{1}{2}\langle P\Psi, QP\Psi \rangle = \frac{1}{2}\langle \Psi, P^*QP\Psi \rangle \equiv \frac{1}{2}\langle \Psi, \mathcal{K}\Psi \rangle, \quad \mathcal{K} = P^*QP. \quad (2.4)$$

In Siegel gauge  $\mathcal{K} = c_0b_0Qb_0c_0 = c_0L_0b_0c_0 = c_0L_0$ . Assuming  $L_0$  has an inverse  $1/L_0$  one can almost invert  $\mathcal{K}$ , except for the fact that  $c_0$  is not invertible. One introduces a propagator  $\mathcal{P}$  such that  $\mathcal{P}\mathcal{K}$  equals the projector to the gauge slice. This is easily done

$$\mathcal{P} = \frac{b_0}{L_0} \quad \text{gives} \quad \mathcal{P}\mathcal{K} = \frac{b_0}{L_0}c_0L_0 = b_0c_0 = P. \quad (2.5)$$

This is reasonable: when solving  $\mathcal{K}\Psi = J$ , the action of  $\mathcal{P}$  on both sides gives  $P\Psi = \mathcal{P}J$  and both left- and right-hand sides are clearly in the gauge.

In Schnabl gauge the kinetic term is

$$\mathcal{K} = P^*QP = -C^*B^*QBC. \quad (2.6)$$

As opposed to the situation in Siegel gauge, this  $\mathcal{K}$  cannot be simplified. The propagator  $\mathcal{P}$  must give  $\mathcal{P}\mathcal{K} = P$ , namely

$$-\mathcal{P}C^*B^*QBC = BC. \quad (2.7)$$

We note that  $\mathcal{P}$  cannot be equal to  $B/L$ . We must have  $\mathcal{P} = B \dots B^*$ , the left-most  $B$  is there to leave us in the gauge ( $B\mathcal{P} = 0$ ) and the right-most  $B^*$  to cancel the  $C^*$  in  $\mathcal{K}$ . As first noticed in [7], the propagator takes the form

$$\mathcal{P} \equiv \frac{B}{L} Q \frac{B^*}{L^*}. \quad (2.8)$$

Indeed, as desired

$$\mathcal{P}\mathcal{K} = -\frac{B}{L} Q \frac{B^*}{L^*} C^*B^*QBC = \frac{B}{L} \frac{Q}{L^*} B^*QBC = \frac{B}{L} QBC = BC. \quad (2.9)$$

One can similarly check that  $\mathcal{K}\mathcal{P} = P^*$ . It is very important to note that the propagator  $\mathcal{P}$  is BPZ even:

$$\begin{aligned} \langle R_{12} | \mathcal{P}^{(1)} &= \langle R_{12} | \frac{B^{(1)}}{L^{(1)}} Q^{(1)} \frac{B^{(1)*}}{L^{(1)*}} = \langle R_{12} | Q^{(1)} \frac{B^{(1)*}}{L^{(1)*}} \frac{B^{(2)*}}{L^{(2)*}} \\ &= \langle R_{12} | (-Q^{(2)}) \frac{B^{(1)*}}{L^{(1)*}} \frac{B^{(2)*}}{L^{(2)*}} \\ &= \langle R_{12} | \frac{B^{(2)}}{L^{(2)}} Q^{(2)} \frac{B^{(2)*}}{L^{(2)*}} = \langle R_{12} | \mathcal{P}^{(2)}. \end{aligned} \quad (2.10)$$

We simply write  $\mathcal{P}^* = \mathcal{P}$ .

The manipulations leading to the derivation of  $\mathcal{P}$  have been somewhat formal – we cancel  $L$ 's against  $1/L$ 's with impunity. As we will see later, there are subtleties that invalidate such cancellations unless a suitably regulated definition of the propagator is used.

## 2.2 CFT representation of $B/L$

Since  $B/L$  and  $B^*/L^*$  enter in the propagator (2.8), we must understand how these operators act on states and their star products. The CFT representation of this action will be used to obtain the string diagrams associated with this gauge. In this subsection we find the CFT representation of the operator  $B/L$ . In the following subsection we study the action of  $B^*/L^*$ .

Let us begin by considering the action of  $1/L$ . For arbitrary Fock space states  $A_1$  and  $A_2$  we have

$$\begin{aligned} \frac{1}{L}(A_1 * A_2) &= \int_0^\infty dT e^{-TL} (A_1 * A_2) = \int_0^\infty dT e^{-TL} A_1 * e^{-T(L-L_L^\dagger)} A_2, \\ &= \int_0^\infty dT e^{-TL} A_1 * e^{(1-e^{-T})L_L^\dagger} e^{-TL} A_2, \\ &= \int_0^1 \frac{dt}{t} t^L A_1 * W_{t-1} * t^L A_2. \end{aligned} \quad (2.11)$$

Here we have used (A.7), (A.10), and  $e^{-\alpha L_L^\dagger} A = W_\alpha * A$ , which holds for arbitrary  $A$ . For multiple string fields this generalizes to

$$\frac{1}{L}(A_1 * A_2 * \dots * A_k) = \int_0^1 \frac{dt}{t} t^L A_1 * (W_{t-1} * t^L A_2) * \dots * (W_{t-1} * t^L A_k). \quad (2.12)$$

There is a wedge  $W_{t-1}$  between every consecutive pair of states  $t^L A_i$  and  $t^L A_{i+1}$ . Given that  $0 \leq t \leq 1$ , this wedge state removes a piece of surface.

It will be convenient to introduce the state  $[A]_t$  associated to the state  $A$  and defined by

$$[A]_t \equiv W_{\frac{1}{2}(t-1)} * t^L A * W_{\frac{1}{2}(t-1)}. \quad (2.13)$$

The state  $[A]_t$  has an interesting geometrical picture, shown in Figure 1. The state  $t^L A$  can be visualized as the unit wedge  $-\frac{1}{2} \leq \text{Re}(z) \leq \frac{1}{2}$ ,  $\text{Im}(z) \geq 0$ , with the operator  $t^L A(\xi = 0)$  mapped to  $z = 0$  by means of

$$z = f(\xi) = \frac{2}{\pi} \tan^{-1} \xi. \quad (2.14)$$

The state  $[A]_t$  is obtained by gluing a wedge of width  $\frac{1}{2}(t-1)$  to the unit-width  $t^L A$  wedge, followed by the gluing of another wedge of width  $\frac{1}{2}(t-1)$ . All together we have a wedge of width  $2 \cdot \frac{1}{2}(t-1) + 1 = t$ . In the CFT language the test state is inserted on the canonical unit wedge and the wedge  $[A]_t$  is built starting at  $z = \frac{1}{2}$ . The local insertion then occurs at  $\frac{1}{2} + \frac{1}{2}(t-1) + \frac{1}{2} = \frac{1}{2}(1+t)$ , so we have

$$\langle \phi, [A]_t \rangle = \langle f \circ \phi(0) f_{\frac{1}{2}(1+t)} \circ t^L A(0) \rangle_{W_t}, \quad (2.15)$$

where

$$f_r(\xi) = r + f(\xi) = T_r \circ f(\xi), \quad \text{with} \quad T_r(z) = z + r. \quad (2.16)$$

Indeed, as constructed, the state  $t^L A$  lands at  $z = \frac{1}{2}(1+t)$  (see Figure 1). The effect of  $t^L$  on the state  $A$  is that of a conformal map, so we can determine what is the full conformal map applied to the state  $A$ . As shown in [14]

$$t^L \phi(\xi) t^{-L} = (f^{-1} \circ t \circ f) \circ \phi(\xi), \quad (2.17)$$



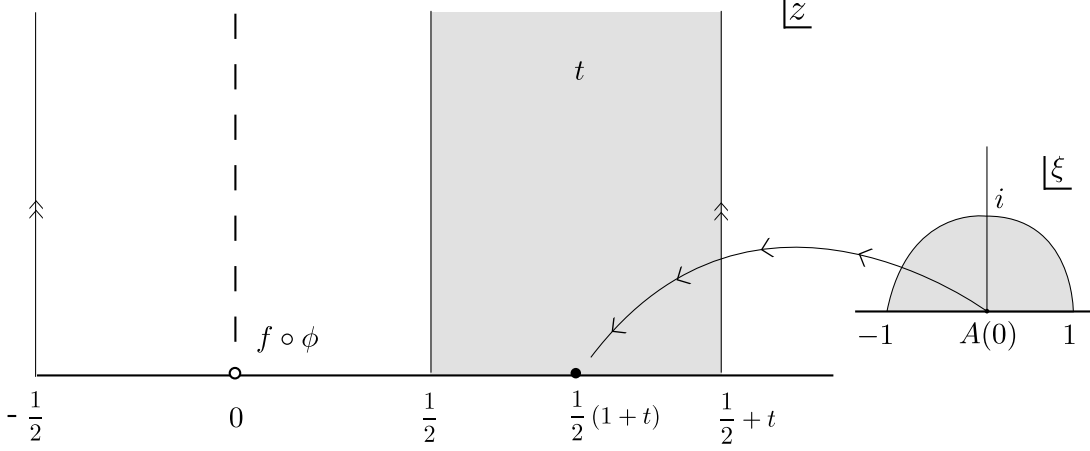


Figure 1: The geometrical picture for the state  $[A]_t$ , a wedge state  $W_t$  with  $A$  inserted using a local coordinate that covers the width  $t$  strip.

where  $t$  denotes the map  $z \rightarrow tz$ . It follows that

$$f_{\frac{1}{2}(1+t)} \circ t^L A(0) = T_{\frac{1}{2}(1+t)} \circ f \circ f^{-1} \circ t \circ f \circ A = T_{\frac{1}{2}(1+t)} \circ t \circ f \circ A. \quad (2.18)$$

As we can see, the effect of  $t^L$  is just to scale the local coordinate by a factor of  $t$ . The local coordinate domain for the  $A$  insertion is thus a wedge of width  $t$ . Since we began with a wedge of unit width, the extra wedge state factors to the left and to the right, provide precisely the missing piece of surface. All in all,

$[A]_t$  is a wedge state of width  $t$  with  $A$  inserted at the boundary midpoint and the local patch filling the wedge.

(2.19)

It follows from (2.13) that

$$t^L A = W_{\frac{1}{2}(1-t)} * [A]_t * W_{\frac{1}{2}(1-t)}. \quad (2.20)$$

We can use this to rewrite (2.12) as

$$\frac{1}{L}(A_1 * A_2 * \dots * A_k) = \int_0^1 \frac{dt}{t} W_{\frac{1}{2}(1-t)} * [A_1]_t * [A_2]_t * \dots * [A_k]_t * W_{\frac{1}{2}(1-t)}. \quad (2.21)$$

The geometrical picture is that of a sequence of glued wedges of width  $t$ , each with a local insertion, flanked from the left and from the right with wedges of size  $\frac{1}{2}(1-t)$ .

Now we proceed with the action of  $B$ , *without* assuming that the states are in Schnabl gauge. We do this on the product of two states, beginning with the result in (2.11). The structure of

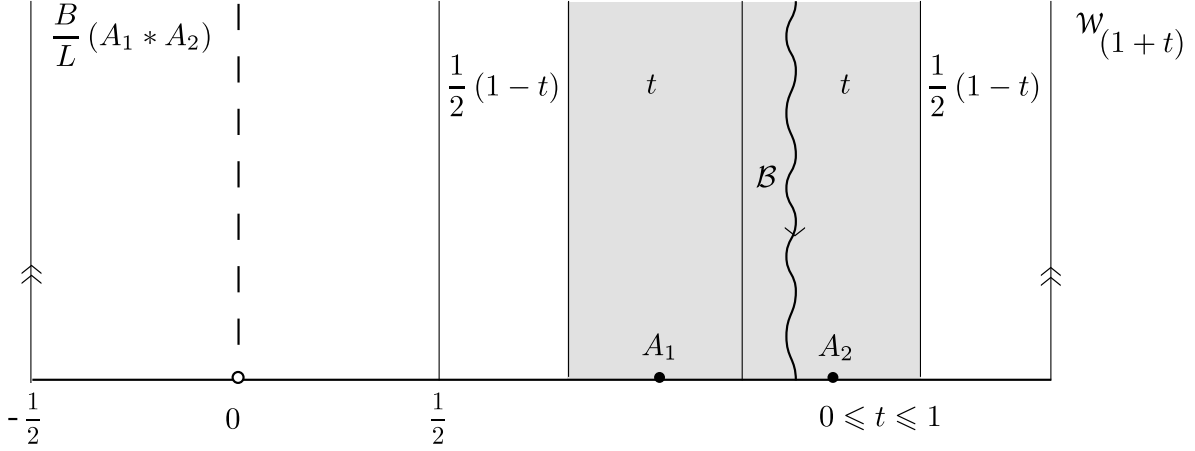


Figure 2: A wedge state in the integral representation (2.26) of  $\frac{B}{L}(A_1 * A_2)$ . Shown is one term only, the other two terms have no  $\mathcal{B}$  insertion but rather local insertions of  $BA_1$  or  $BA_2$ . Note the wedges of width  $\frac{1}{2}(1-t)$ , with  $t \in [0, 1]$ , to the sides of  $[A_1]_t * [A_2]_t$ .

terms requires the evaluation of

$$M \equiv (B - B_L^+)W_{t-1} * t^L A_2 + W_{t-1} * (B - B_L^+)t^L A_2. \quad (2.22)$$

Using  $(B - B_L^+)W_\alpha = -\alpha B_L^+ W_\alpha$ , we get

$$M = -tB_L^+ W_{t-1} * t^L A_2 + W_{t-1} * t^L B A_2. \quad (2.23)$$

The calculation is then straightforward

$$\begin{aligned} \frac{B}{L}(A_1 * A_2) = \int_0^1 \frac{dt}{t} \left[ t^L B A_1 * W_{t-1} * t^L A_2 \right. \\ \left. + (-1)^{A_1+1} t^{L+1} A_1 * B_L^+ W_{t-1} * t^L A_2 \right. \\ \left. + (-1)^{A_1} t^L A_1 * W_{t-1} * t^L B A_2 \right]. \end{aligned} \quad (2.24)$$

Rearranging we get

$$\begin{aligned} \frac{B}{L}(A_1 * A_2) = (-1)^{A_1+1} \int_0^1 dt t^L A_1 * B_L^+ W_{t-1} * t^L A_2 \\ + \int_0^1 \frac{dt}{t} \left[ t^L B A_1 * W_{t-1} * t^L A_2 + (-1)^{A_1} t^L A_1 * W_{t-1} * t^L B A_2 \right]. \end{aligned} \quad (2.25)$$

In terms of states of type  $[\dots]$ ,

$$\begin{aligned} \frac{B}{L}(A_1 * A_2) = (-1)^{A_1+1} \int_0^1 dt W_{\frac{1}{2}(1-t)} * [A]_t * B_L^+ [A_2]_t * W_{\frac{1}{2}(1-t)} \\ + \int_0^1 \frac{dt}{t} W_{\frac{1}{2}(1-t)} * \left[ [B A_1]_t * [A_2]_t + (-1)^{A_1} [A_1]_t * [B A_2]_t \right] * W_{\frac{1}{2}(1-t)}. \end{aligned} \quad (2.26)$$

The first line on the right-hand side of (2.26) is represented in Figure 2. This expression makes it manifest that the local coordinate patches of  $A_1$  and  $A_2$  match seamlessly. Moreover, extra strips of width  $\frac{1}{2}(1-t)$  are added to the left and to the right of the  $[A]_t$  and  $[A]_2$  wedges, as shown in the figure. For one state only we have

$$\frac{B}{L}A = \int_0^1 \frac{dt}{t} W_{\frac{1}{2}(1-t)} * [BA]_t * W_{\frac{1}{2}(1-t)}. \quad (2.27)$$

### 2.3 CFT representation of $B^*/L^*$

We begin with the evaluation of  $1/L^*$  acting on a single state:

$$\frac{1}{L^*}A = \int_0^\infty dT e^{-TL^*} A = \int_0^\infty dT e^{-T(L^+-L)} A. \quad (2.28)$$

The exponential can be broken up using (A.9):

$$\frac{1}{L^*}A = \int_0^\infty dT e^{(1-e^T)L^+} e^{TL} A = \int_1^\infty \frac{ds}{s} e^{(1-s)L^+} s^L A \quad (2.29)$$

$$\frac{1}{L^*}A = \int_1^\infty \frac{ds}{s} W_{s-1} * s^L A * W_{s-1}. \quad (2.30)$$

To generalize we recall the second identity in (A.7), and noting that  $L^* - L_L^+ = L_R^+ - L$ , we get

$$e^{-TL^*}(\phi_1 * \phi_2 * \dots * \phi_n) = e^{-TL^*} \phi_1 * e^{T(L-L_R^+)} \phi_2 * \dots * e^{T(L-L_R^+)} \phi_n. \quad (2.31)$$

With this and (A.11) we find

$$\begin{aligned} \frac{1}{L^*}(A_1 * A_2 * \dots * A_k) &= \int_0^\infty dT e^{-TL^*} A_1 * e^{T(L-L_R^+)} A_2 * \dots * e^{T(L-L_R^+)} A_k \quad (2.32) \\ &= \int_0^\infty dT e^{(1-e^T)L^+} e^{TL} A_1 * e^{-(e^T-1)L_R^+} e^{TL} A_2 * \dots * e^{-(e^T-1)L_R^+} e^{TL} A_k \\ &= \int_1^\infty \frac{ds}{s} e^{(1-s)L^+} s^L A_1 * e^{-(s-1)L_R^+} s^L A_2 * \dots * e^{-(s-1)L_R^+} s^L A_k. \end{aligned}$$

Therefore we have:

$$\frac{1}{L^*}(A_1 * A_2 * \dots * A_k) = \int_1^\infty \frac{ds}{s} W_{s-1} * s^L A_1 * W_{s-1} * s^L A_2 * \dots * W_{s-1} * s^L A_k * W_{s-1}. \quad (2.33)$$

It is interesting to compare with (2.12). There are two differences. First,  $1/L^*$  produces two extra factors of  $W_{s-1}$ , one to the left and one to the right of the sequence of states. Second, the range of integration is different. While  $1/L$  induces contractions ( $t \leq 1$ ),  $1/L^*$  induces expansion ( $s \geq 1$ ). In the language of overlap states

$$\frac{1}{L^*}(A_1 * A_2 * \dots * A_k) = \int_1^\infty \frac{ds}{s} W_{\frac{1}{2}(s-1)} * [A_1]_s * [A_2]_s * \dots * [A_k]_s * W_{\frac{1}{2}(s-1)}. \quad (2.34)$$

The off-shell states have been expanded and there are wedges flanking the result from the left and from the right.

The calculation of the  $B^*$  action requires a few formulas. Given the  $B^*$  action (A.6) on star products, one needs the action of  $B^*$  and  $B^* - B_L^+$  on wedge states, as given in (A.25, A.26). Given the structure of terms in (2.33) we require the evaluation of

$$M' \equiv (B^* - B_L^+)s^L A * W_{s-1} + (-1)^A s^L A * (B^* - B_L^+)W_{s-1}. \quad (2.35)$$

In the first factor we replace  $B^* - B_L^+ = B_R^+ - B$  and in the second we use the  $B^* - B_L^+$  action on wedge states,

$$M' = (B_R^+ - B)s^L A * W_{s-1} + (-1)^A (s-1) s^L A * B_L^+ W_{s-1}. \quad (2.36)$$

The  $B_R^+$  in the first term can be moved to act on  $W_{s-1}$  and the resulting term combines with the second term:

$$M' = -s^L B A * W_{s-1} + (-1)^A s^L A * B_L^+ W_{s-1}. \quad (2.37)$$

We can now begin the calculation of

$$\frac{B^*}{L^*}(A_1 * A_2) = \int_1^\infty \frac{ds}{s} B^*(W_{s-1} * s^L A_1 * W_{s-1} * s^L A_2 * W_{s-1}). \quad (2.38)$$

Since  $B^* W_{s-1} = s B_L^+ W_{s-1}$  we get

$$\begin{aligned} \frac{B^*}{L^*}(A_1 * A_2) &= \int_1^\infty ds \left[ B_L^+ W_{s-1} * s^L A_1 * W_{s-1} * s^L A_2 * W_{s-1} \right. \\ &\quad + (-1)^{A_1} W_{s-1} * s^L A_1 * B_L^+ W_{s-1} * s^L A_2 * W_{s-1} \\ &\quad \left. + (-1)^{A_1+A_2} W_{s-1} * s^L A_1 * W_{s-1} * s^L A_2 * B_L^+ W_{s-1} \right] \\ &\quad - \int_1^\infty \frac{ds}{s} W_{s-1} * \left[ s^L B A_1 * W_{s-1} * s^L A_2 + (-1)^{A_1} s^L A_1 * W_{s-1} * s^L B A_2 \right] * W_{s-1}. \end{aligned} \quad (2.39)$$

In the overlap notation, we have

$$\begin{aligned} \frac{B^*}{L^*}(A_1 * A_2) &= \int_1^\infty ds \left[ B_L^+ W_{\frac{1}{2}(s-1)} * [A_1]_s * [A_2]_s * W_{\frac{1}{2}(s-1)} \right. \\ &\quad + (-1)^{A_1} W_{\frac{1}{2}(s-1)} * [A_1]_s * B_L^+ [A_2]_s * W_{\frac{1}{2}(s-1)} \\ &\quad \left. + (-1)^{A_1+A_2} W_{\frac{1}{2}(s-1)} * [A_1]_s * [A_2]_s * B_L^+ W_{\frac{1}{2}(s-1)} \right] \\ &\quad - \int_1^\infty \frac{ds}{s} \left[ W_{\frac{1}{2}(s-1)} * [B A_1]_s * [A_2]_s * W_{\frac{1}{2}(s-1)} \right. \\ &\quad \left. + (-1)^{A_1} W_{\frac{1}{2}(s-1)} * [A_1]_s * [B A_2]_s * W_{\frac{1}{2}(s-1)} \right]. \end{aligned} \quad (2.40)$$

The second line on the right-hand side is illustrated in Figure 3.

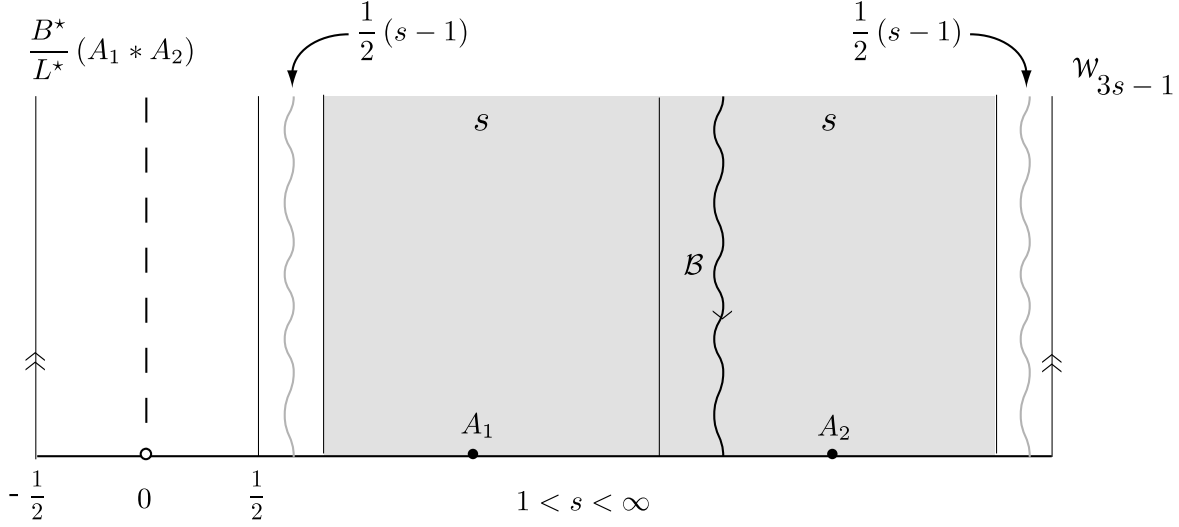


Figure 3: A term in the representation (2.40) of  $\frac{B^*}{L^*}(A_1 * A_2)$ . Two similar terms in (2.40) have the  $\mathcal{B}$  insertion at the positions shown in gray. The two remaining terms have no  $\mathcal{B}$  but rather local insertions of  $BA_1$  or  $BA_2$ . Wedges of width  $\frac{1}{2}(s-1)$ , with  $s \in [1, \infty)$ , flank  $[A_1]_s * [A_2]_s$ .

### 3 The off-shell Veneziano amplitude: first two diagrams

The four point amplitude is obtained by joining two cubic vertices with a propagator. For arbitrary states  $\Psi_i$  ordered as 1234 along the boundary, the  $s$ -channel contribution is given by

$$\mathcal{F}_s = \left\langle \Psi_1 * \Psi_2, \mathcal{P}(\Psi_3 * \Psi_4) \right\rangle. \quad (3.1)$$

Since  $\mathcal{P}$  is BPZ even,  $\mathcal{F}_s$  is symmetric under the exchange of  $(\Psi_1, \Psi_2) \leftrightarrow (\Psi_3, \Psi_4)$ . One's first instinct is to process  $\mathcal{F}_s$  by moving the BRST operator in  $\mathcal{P}$  to the right,

$$\mathcal{P} \stackrel{?}{=} \frac{B}{L} - \frac{B B^*}{L L^*} Q. \quad (3.2)$$

Then

$$\mathcal{F}_s \stackrel{?}{=} \mathcal{F}^{(1)} + \mathcal{F}^{(2)} + \mathcal{F}^{(2')}, \quad (3.3)$$

with

$$\begin{aligned} \mathcal{F}^{(1)} &\equiv \left\langle \Psi_1 * \Psi_2, \frac{B}{L}(\Psi_3 * \Psi_4) \right\rangle, \\ \mathcal{F}^{(2)} &\equiv -\left\langle \Psi_1 * \Psi_2, \frac{B B^*}{L L^*}(Q\Psi_3 * \Psi_4) \right\rangle, \\ \mathcal{F}^{(2')} &\equiv \left\langle \Psi_1 * \Psi_2, \frac{B B^*}{L L^*}(\Psi_3 * Q\Psi_4) \right\rangle. \end{aligned} \quad (3.4)$$

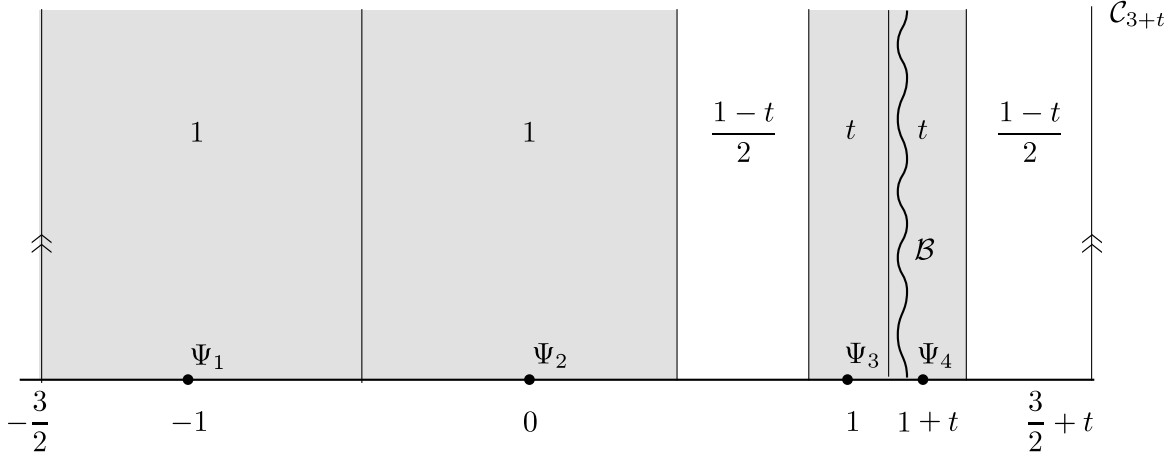


Figure 4: The first string diagram  $\mathcal{F}^{(1)}$ , with  $t \in [0, 1]$ . For  $t = 0$  punctures 3 and 4 collide. For  $t = 1$  the punctures are uniformly spaced on the boundary.

In this section we evaluate  $\mathcal{F}^{(1)}$  (the “first diagram”) and  $\mathcal{F}^{(2)} + \mathcal{F}^{(2')}$  (the “second diagram”) for external off-shell tachyons. We shall find that  $\mathcal{F}^{(1)} + \mathcal{F}^{(2)} + \mathcal{F}^{(2')}$  is not symmetric under the exchange  $12 \leftrightarrow 34$  – in contradiction with the symmetry of the starting point (3.1). To the rescue will come a boundary term, discussed at length in the next section.

As usual, we will use the Mandelstam variables:

$$\mathbf{s} = -(p_1 + p_2)^2, \quad \mathbf{t} = -(p_2 + p_3)^2, \quad \mathbf{u} = -(p_1 + p_3)^2, \quad \mathbf{s} + \mathbf{t} + \mathbf{u} = -\sum p_i^2. \quad (3.5)$$

### 3.1 First diagram

Using (2.26), recalling that  $(-B_L^+)$  is represented by the insertion of  $\mathcal{B}$ , and noting that the external states are all annihilated by  $B$ , the first diagram  $\mathcal{F}^{(1)}$  is given by

$$\mathcal{F}^{(1)} = -\int_0^1 dt \left\langle [\Psi_1]_1 * [\Psi_2]_1, W_{\frac{1}{2}(1-t)} * [\Psi_3]_t * \mathcal{B}[\Psi_4]_t * W_{\frac{1}{2}(1-t)} \right\rangle. \quad (3.6)$$

The string diagram is the cylinder of total width  $3 + t$  shown in Figure 4. Note that states 1 and 2 appear on wedges of unit width, while states 3 and 4 appear on wedges of width  $t$ . We consider general external states of the form

$$|\Psi_i\rangle = V_i c_1 |0\rangle, \quad (3.7)$$

where  $V_i$  are matter primary operators of dimension  $\Delta_i$ . We have

$$L|\Psi_i\rangle = (\Delta_i - 1)|\Psi_i\rangle, \quad Q|\Psi_i\rangle = (\Delta_i - 1)V_i c_0 c_1 |0\rangle. \quad (3.8)$$

The conformal map of  $\Psi_i$  by

$$z = t \frac{2}{\pi} \tan^{-1}(\xi) \quad (3.9)$$

implies that  $[\Psi_i]_t$  is represented by the local insertion of  $\left(\frac{2t}{\pi}\right)^{\Delta_i-1} \Psi_i(z_i)$ . Thus we find

$$\mathcal{F}^{(1)} = -\left(\frac{\pi}{2}\right)^{4-\Delta_i} \int_0^1 \frac{dt}{t^{2-\Delta_3-\Delta_4}} \left\langle cV_1(-1) cV_2(0) cV_3(1) \mathcal{B} cV_4(1+t) \right\rangle_{\mathcal{C}_{3+t}}. \quad (3.10)$$

The CFT correlator factorizes into a matter part times a ghost part. It is convenient to use cyclicity and the identification  $z \sim z + 3 + t$  to rewrite the ghost correlator as

$$\left\langle c(-1) c(0) c(1) \mathcal{B} c(1+t) \right\rangle_{\mathcal{C}_{3+t}} = \left\langle \mathcal{B} c(-2) c(-1) c(0) c(1) \right\rangle_{\mathcal{C}_{3+t}}. \quad (3.11)$$

This is immediately evaluated using (B.39). Making also use of the trigonometric identity  $3 \sin x - \sin(3x) = 4 \sin^3 x$  we find

$$\left\langle \mathcal{B} c(-2) c(-1) c(0) c(1) \right\rangle_{\mathcal{C}_{3+t}} = -\frac{4}{\pi^3} (3+t)^2 \sin\left[\frac{2\pi}{3+t}\right] \sin^4\left[\frac{\pi}{3+t}\right]. \quad (3.12)$$

To evaluate the matter correlator, we specialize to tachyon vertex operators:

$$V_i = e^{\alpha' p_i X}, \quad \Delta_i = \alpha' p_i^2. \quad (3.13)$$

Using (B.41) we find that

$$\begin{aligned} \left\langle e^{ip_1 \cdot X(-1)} e^{ip_2 \cdot X(0)} e^{ip_3 \cdot X(1)} e^{ip_4 \cdot X(1+t)} \right\rangle_{\mathcal{C}_{3+t}} &= (2\pi)^D \delta\left(\sum p_i\right) \left(\frac{3+t}{\pi}\right)^{-\alpha' \sum p_i^2} \\ &\cdot \left(\sin\left[\frac{\pi}{3+t}\right]\right)^{-\alpha'(2t+s+p_1^2+p_2^2+\sum p_i^2)} \left(\sin\left[\frac{2\pi}{3+t}\right]\right)^{\alpha'(2s+2t+\sum p_i^2)} \left(\sin\left[\frac{3\pi}{3+t}\right]\right)^{-\alpha'(s+p_4^2+p_3^2)}. \end{aligned} \quad (3.14)$$

Assembling our results back into (3.10) we have

$$\begin{aligned} \mathcal{F}^{(1)} &= \frac{4}{\pi} \left(\frac{\pi}{2}\right)^{4-\alpha' \sum p_i^2} (2\pi)^D \delta\left(\sum p_i\right) \int_0^1 \frac{dt}{t^{2-\alpha'(p_3^2+p_4^2)}} \left(\frac{3+t}{\pi}\right)^{2-\alpha' \sum p_i^2} \left(\sin\left[\frac{3\pi}{3+t}\right]\right)^{-\alpha'(s+p_4^2+p_3^2)} \\ &\cdot \left(\sin\left[\frac{\pi}{3+t}\right]\right)^{4-\alpha'(2t+s+p_1^2+p_2^2+\sum p_i^2)} \cdot \left(\sin\left[\frac{2\pi}{3+t}\right]\right)^{1+\alpha'(2s+2t+\sum p_i^2)}. \end{aligned} \quad (3.15)$$

It is useful to make a change of variables from  $t$  to a more relevant variable – the modulus  $\lambda$  of the four-punctured disk. Let us then review how to calculate the modulus  $\lambda$  of a disk with four punctures  $P_1, P_2, P_3$ , and  $P_4$  located with clockwise ordering on the boundary of the disk. The modulus  $\lambda$ , with  $0 \leq \lambda \leq 1$ , is defined as the coordinate of  $P_2$  after a map to the upper-half

plane in which  $P_1, P_2$ , and  $P_3$  go to 0, 1, and  $\infty$ , respectively. Our disk is presented as a circular unit disk and the relevant information is the angular separations between the punctures. We introduce the angle variable  $\theta_{ij}$  with  $i < j$  to denote the positive angle of rotation that is needed to go from  $P_i$  to  $P_j$ . The relevant configuration is shown in Figure 5. With  $w$  denoting the coordinate on the disk, a map to the upper-half plane is

$$z = \frac{1}{i} \frac{w - 1}{w + 1}. \quad (3.16)$$

One can readily verify that for points  $w = e^{i\theta}$  on the boundary of the disk

$$z(w = e^{i\theta}) = \tan \frac{\theta}{2}. \quad (3.17)$$

Placing  $P_1$  at  $w = 1$ , the punctures  $P_i$  are mapped to  $z_i$  where

$$z_1 = 0, \quad z_2 = \tan \frac{\theta_{12}}{2}, \quad z_3 = \tan \frac{\theta_{13}}{2}, \quad z_4 = \tan \frac{\theta_{14}}{2}. \quad (3.18)$$

The modulus  $\lambda$  is then

$$\lambda = \frac{(z_1 - z_2)(z_3 - z_4)}{(z_1 - z_3)(z_2 - z_4)} = \frac{z_2(z_3 - z_4)}{z_3(z_2 - z_4)}. \quad (3.19)$$

A short calculation using the values indicated in (3.18) gives the final result

$$\lambda = \frac{\sin\left(\frac{\theta_{12}}{2}\right) \sin\left(\frac{\theta_{34}}{2}\right)}{\sin\left(\frac{\theta_{13}}{2}\right) \sin\left(\frac{\theta_{24}}{2}\right)}. \quad (3.20)$$

To apply this result to cylinder diagrams we note that the angle between two punctures is simply given by  $2\pi$  times the ratio of the separation between the punctures and the total circumference.

We apply (3.20) to the first string diagram (Figure 4) and find that the modulus  $\lambda$  is the given by

$$\lambda = \frac{\sin\left[\frac{\pi}{3+t}\right] \sin\left[\frac{\pi t}{3+t}\right]}{\sin^2\left[\frac{2\pi}{3+t}\right]}. \quad (3.21)$$

We readily check that this result correctly implies that  $\lambda(t = 0) = 0$ , since then punctures 3 and 4 collide, which is conformally equivalent to the collision of punctures 1 and 2. We also check that  $\lambda(t = 1) = 1/2$ , which corresponds to the configuration of equally spaced punctures on the boundary of the disk. Using trigonometric identities we find the alternative useful formulas

$$4 \sin^2\left[\frac{\pi}{3+t}\right] = \frac{3 - 4\lambda}{1 - \lambda}, \quad \cos^2\left[\frac{\pi}{3+t}\right] = \frac{1}{4} \cdot \frac{1}{1 - \lambda}, \quad (3.22)$$

as well as the Jacobian

$$\frac{4}{\pi} \frac{\pi^2}{(3+t)^2} \sin\left[\frac{2\pi}{3+t}\right] dt = \frac{d\lambda}{(1-\lambda)^2}, \quad (3.23)$$



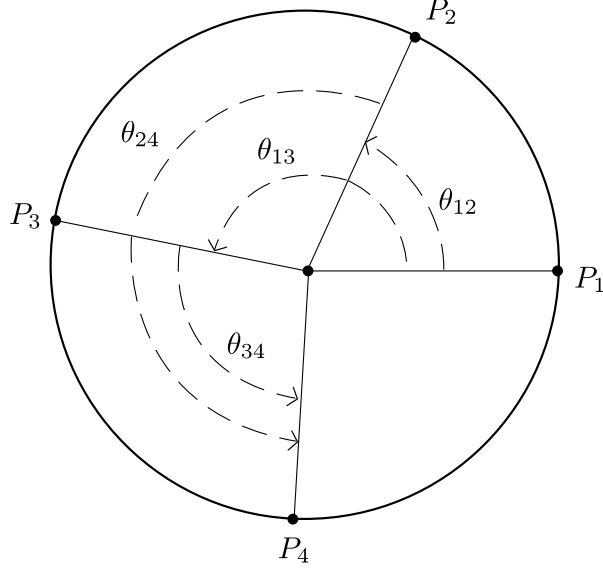


Figure 5: A disk with four punctures  $P_i$ ,  $i = 1, 2, 3, 4$ . The angle  $\theta_{ij}$ , with  $i < j$  is defined as the (lowest) clockwise rotation angle that takes  $P_i$  to  $P_j$ .

which also implies that for small  $\lambda$  and small  $t$  we have

$$\frac{\lambda}{t} \rightarrow \frac{2\pi}{3\sqrt{3}}. \quad (3.24)$$

Using  $\lambda$  as integration variable the full amplitude (3.15) becomes

$$\begin{aligned} \mathcal{F}^{(1)} = & (2\pi)^D \delta\left(\sum p_i\right) \int_0^{1/2} d\lambda (1-\lambda)^{-2} \left(\sin\left[\frac{3\pi}{3+t}\right]\right)^{-\alpha'(s+p_4^2+p_3^2)} \\ & \cdot \left(\sin\left[\frac{\pi}{3+t}\right]\right)^{4-\alpha'(2t+s+p_1^2+p_2^2+\sum p_i^2)} \cdot \left(\sin\left[\frac{2\pi}{3+t}\right]\right)^{\alpha'(2s+2t+\sum p_i^2)} \\ & \cdot \left(\frac{\pi}{2}\right)^{4-\alpha'\sum p_i^2} \left(\frac{3+t}{\pi}\right)^{4-\alpha'\sum p_i^2} \frac{1}{t^{2-\alpha'(p_3^2+p_4^2)}}. \end{aligned} \quad (3.25)$$

Making use of the identities

$$\begin{aligned} \sin\left[\frac{\pi}{3+t}\right] &= (1-\lambda)^{-1/2} \left(\frac{3}{4}-\lambda\right)^{1/2}, \\ \sin\left[\frac{2\pi}{3+t}\right] &= (1-\lambda)^{-1} \left(\frac{3}{4}-\lambda\right)^{1/2}, \\ \sin\left[\frac{3\pi}{3+t}\right] &= \lambda(1-\lambda)^{-3/2} \left(\frac{3}{4}-\lambda\right)^{1/2}, \end{aligned} \quad (3.26)$$

a calculation gives the relatively simple result

$$\begin{aligned} \mathcal{F}^{(1)} = & (2\pi)^D \delta\left(\sum p_i\right) \int_0^{1/2} d\lambda \lambda^{-\alpha's-2} (1-\lambda)^{-\alpha't-2} \\ & \cdot \left[\frac{1}{2}(3+t) \sin\left[\frac{2\pi}{3+t}\right]\right]^x \left[\frac{\lambda}{t}\right]^{\chi_{34}} (1-\lambda)^{\chi_{12}}, \end{aligned} \quad (3.27)$$

where we have defined variables  $\chi_{ij}$  and  $\chi$  that vanish on-shell:

$$\boxed{\chi_{ij} \equiv 2 - \alpha'(p_i^2 + p_j^2), \quad \chi = 4 - \alpha' \sum_{i=1}^4 p_i^2.} \quad (3.28)$$

In (3.27) one views  $t$  as a function of  $\lambda$ , as defined by (3.22). An alternative expression is

$$\boxed{\mathcal{F}^{(1)} = (2\pi)^D \delta\left(\sum p_i\right) \int_0^{1/2} d\lambda \lambda^{-\alpha's-2} (1-\lambda)^{-\alpha't-2} \cdot \left[\frac{\pi}{2}(1-\lambda)^{1/2} \cdot \frac{3+t}{\pi} \sin\left[\frac{\pi}{3+t}\right]\right]^\chi \left[\frac{\lambda}{t(1-\lambda)}\right]^{\chi_{34}}.} \quad (3.29)$$

Note that on-shell the second line in the above result gives a factor of one. The first line then gives us the familiar on-shell Veneziano amplitude. Of course, one must still add the contribution from the  $\mathbf{t}$ -channel diagram to obtain the region of integration  $\lambda \in [0, 1]$  and then the contribution from other cyclic orderings of the punctures. Since we have shown that this first diagram gives the correct on-shell amplitude, it is clear that the contributions from the remaining diagrams should vanish on-shell.

We can use (3.29) to obtain the form of the amplitude near the pole at  $\alpha's + 1 = 0$ . For this we simply expand for  $\lambda$  near zero and use (3.24) to obtain

$$\mathcal{F}^{(1)}|_{pole} \simeq (2\pi)^D \delta\left(\sum p_i\right) \left[-\frac{1}{\alpha's + 1}\right] \cdot \left[\frac{3\sqrt{3}}{4}\right]^\chi \left[\frac{2\pi}{3\sqrt{3}}\right]^{\chi_{34}}, \quad (3.30)$$

or just

$$\mathcal{F}^{(1)}|_{pole} \simeq (2\pi)^D \delta\left(\sum p_i\right) \left[-\frac{1}{\alpha's + 1}\right] \cdot \left[\frac{3\sqrt{3}}{4}\right]^{\chi_{12}} \left[\frac{\pi}{2}\right]^{\chi_{34}}. \quad (3.31)$$

The external states 1 and 2 appear with the expected off-shell factor of the Witten vertex. States 3 and 4, which collide in the string diagram, carry a different off-shell factor. This happens because  $B/L$  is not BPZ symmetric.

We can now ask: To include the contribution from the  $\mathbf{t}$ -channel diagram can we simply extend the region of integration in (3.29) from  $\lambda \in [0, 1/2]$  to  $\lambda \in [0, 1]$ ? Though this would work on-shell, it does not work off-shell. In fact, the second line in (3.29) does not make sense beyond  $\lambda = 3/4$ , as can be seen from the top equation in (3.26). The value  $\lambda = 3/4$  corresponds to the maximum modulus that can be attained in this string diagram: the modulus for  $t \rightarrow \infty$ .

The  $\mathbf{t}$ -channel answer is obtained by noting that the corresponding diagram arises from (3.1) by the replacements  $\Psi_1 \rightarrow \Psi_2$ ,  $\Psi_2 \rightarrow \Psi_3$ ,  $\Psi_3 \rightarrow \Psi_4$  and  $\Psi_4 \rightarrow \Psi_1$ . This has the effect

of exchanging  $\mathbf{s}$  and  $\mathbf{t}$  and replacing  $\chi_{ij} \rightarrow \chi_{i+1,j+1}$  (understanding that subscripts are defined mod 4). We rewrite the  $\mathbf{s}$ -channel contribution (3.29) as

$$\mathcal{F}_{\mathbf{s}}^{(1)} = (2\pi)^D \delta\left(\sum p_i\right) \int_0^{1/2} d\lambda \lambda^{-\alpha' \mathbf{s}-2} (1-\lambda)^{-\alpha' \mathbf{t}-2} \left[h_1(\lambda)\right]^x \left[h_2(\lambda)\right]^{x_{34}}, \quad (3.32)$$

adding the subscript  $\mathbf{s}$  to denote that this is the  $\mathbf{s}$ -channel contribution and introducing functions  $h_1$  and  $h_2$  that can be easily read from (3.29). The contribution from the  $\mathbf{t}$ -channel would be

$$\mathcal{F}_{\mathbf{t}}^{(1)} = (2\pi)^D \delta\left(\sum p_i\right) \int_0^{1/2} d\lambda \lambda^{-\alpha' \mathbf{t}-2} (1-\lambda)^{-\alpha' \mathbf{s}-2} \left[h_1(\lambda)\right]^x \left[h_2(\lambda)\right]^{x_{41}}. \quad (3.33)$$

Letting  $\lambda \rightarrow 1 - \lambda$ , we find

$$\mathcal{F}_{\mathbf{t}}^{(1)} = (2\pi)^D \delta\left(\sum p_i\right) \int_{1/2}^1 d\lambda \lambda^{-\alpha' \mathbf{s}-2} (1-\lambda)^{-\alpha' \mathbf{t}-2} \left[h_1(1-\lambda)\right]^x \left[h_2(1-\lambda)\right]^{x_{41}}. \quad (3.34)$$

Together,  $\mathcal{F}_{\mathbf{s}}^{(1)}$  and  $\mathcal{F}_{\mathbf{t}}^{(1)}$  cover the modular region  $\lambda \in [0, 1]$ . It is an important consistency condition on the off-shell amplitude that the integrands of  $\mathcal{F}_{\mathbf{s}}^{(1)}$  and  $\mathcal{F}_{\mathbf{t}}^{(1)}$  match at the boundary point  $\lambda = 1/2$ . This matching occurs for arbitrary value of  $h_1(1/2)$  but requires  $h_2(1/2) = 1$ . Happily, this is the case because  $\lambda = 1/2$  corresponds to  $t = 1$ .

## 3.2 Second diagram

The formulas developed so far are in principle sufficient to evaluate  $\mathcal{F}^{(2)}$  and  $\mathcal{F}^{(2)'}$  in (3.15). Using BPZ conjugation, we could write

$$\mathcal{F}^{(2)} = -\left\langle \frac{B^*}{L^*}(\Psi_1 * \Psi_2), \frac{B^*}{L^*}(Q\Psi_3 * \Psi_4) \right\rangle, \quad (3.35)$$

and proceed by computing the action of  $B^*/L^*$  on the two star products. The resulting expression is the sum of ten inequivalent terms and would be rather lengthy to evaluate. Instead, we are going to use a simpler method inspired by a similar treatment in [32].

Since we have seen that the action of  $B/L$  on star products is somewhat simpler than the action of  $B^*/L^*$ , it is advantageous to reorder

$$\frac{B}{L} \frac{B^*}{L^*} = \int_0^\infty dT_1 dT_2 B e^{-T_1 L} e^{-T_2 L^*} B^* \quad (3.36)$$

in such a way that the  $L$  and  $B$  operators are moved to the right of the  $L^*$  and  $B^*$  operators. In appendix C we prove the elegant rearrangement formula

$$\boxed{\frac{B}{L} \frac{B^*}{L^*} = - \int_{\mathcal{M}} d\tau_1 d\tau_2 B^* e^{-\tau_2 L^*} B e^{-\tau_1 L},} \quad (3.37)$$

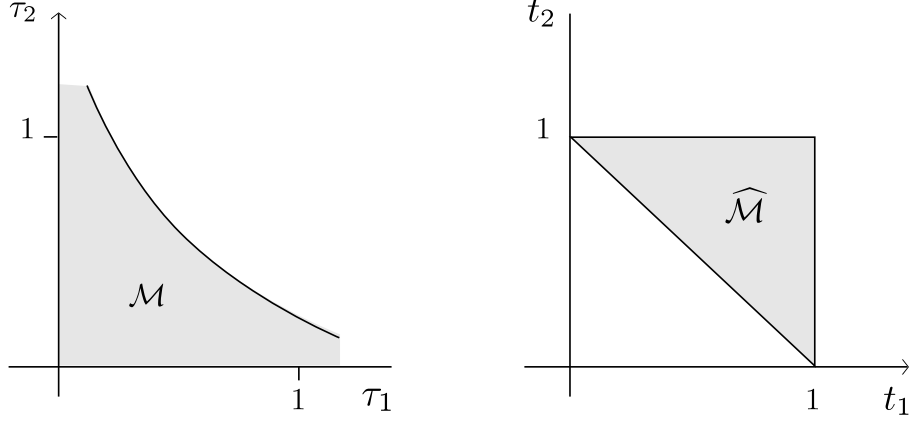


Figure 6: Left: region of integration on the right-hand side of the rearrangement formula (3.37). Right: The same region of integration in triangular variables.

where the region of integration  $\mathcal{M}$  is defined by

$$\mathcal{M} \equiv \{\tau_1, \tau_2 \mid \tau_1 \geq 0, \tau_2 \geq 0, e^{-\tau_1} + e^{-\tau_2} \geq 1\}. \quad (3.38)$$

The region  $\mathcal{M}$  is shown in the left part of Figure 6. Note that if the integration were over the whole range of positive  $\tau_1$  and  $\tau_2$ , the right-hand side of (3.37) would be equal to  $-\frac{B^* B}{L^* L}$ .

With the use of the rearrangement formula the contributions (3.4) to the second diagram can be written as

$$\mathcal{F}^{(2)} = \int_{\mathcal{M}} d\tau_1 d\tau_2 \left\langle B e^{-\tau_2 L} (\Psi_1 * \Psi_2), B e^{-\tau_1 L} (Q \Psi_3 * \Psi_4) \right\rangle. \quad (3.39)$$

$$\mathcal{F}^{(2)} = - \int_{\mathcal{M}} d\tau_1 d\tau_2 \left\langle B e^{-\tau_2 L} (\Psi_1 * \Psi_2), B e^{-\tau_1 L} (\Psi_3 * Q \Psi_4) \right\rangle. \quad (3.40)$$

Evaluating the action of  $B e^{-\tau L}$  on the star products by the techniques of §2, and using  $t_1 = e^{-\tau_1}$ ,  $t_2 = e^{-\tau_2}$ , we find

$$\begin{aligned} \mathcal{F}^{(2)} = \int_{\widehat{\mathcal{M}}} dt_1 dt_2 \left\langle W_{\frac{1}{2}(1-t_2)} * [\Psi_1]_{t_2} * B_L^+ [\Psi_2]_{t_2} * W_{\frac{1}{2}(1-t_2)}, \right. \\ \left. - W_{\frac{1}{2}(1-t_1)} * [Q \Psi_3]_{t_1} * B_L^+ [\Psi_4]_{t_1} * W_{\frac{1}{2}(1-t_1)} + \frac{1}{t_1} W_{\frac{1}{2}(1-t_1)} * [B Q \Psi_3]_{t_1} * [\Psi_4]_{t_1} * W_{\frac{1}{2}(1-t_1)} \right\rangle, \end{aligned} \quad (3.41)$$

where the region of integration is the triangular region

$$\widehat{\mathcal{M}} \equiv \{t_1, t_2 \mid 0 \leq t_1 \leq 1, 0 \leq t_2 \leq 1, t_1 + t_2 \geq 1\}, \quad (3.42)$$

shown on the right part of Figure 6. The string diagram for the first contribution in (3.41) is shown as a cylinder of width  $2 + t_1 + t_2$  in Figure 10.

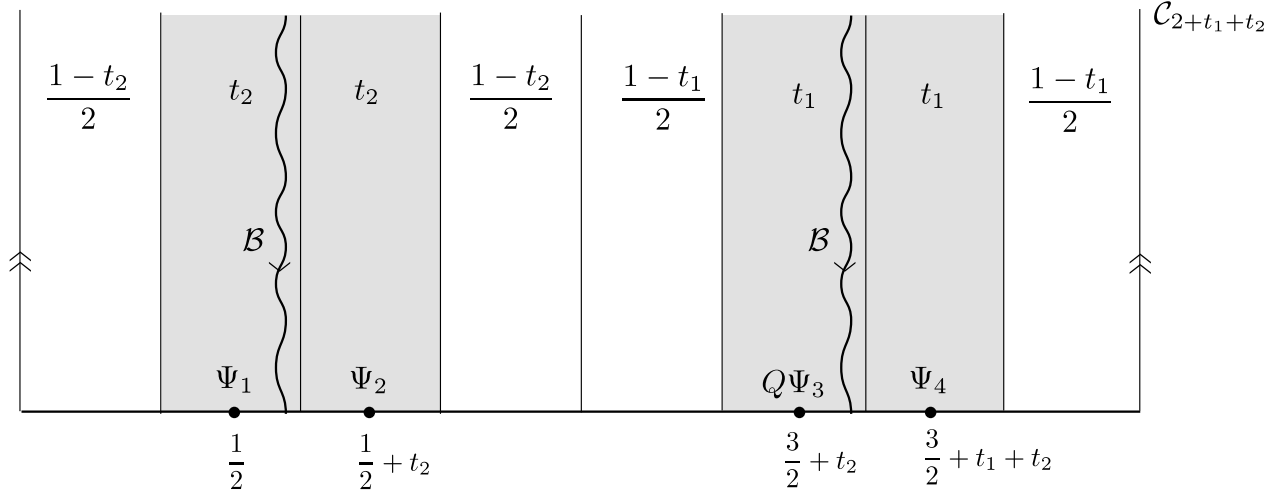


Figure 7: One of the terms in the second string diagram.

Taking states of the from  $\Psi_i = cV_i$ , we find

$$\mathcal{F}^{(2)} = - \int_{\widehat{\mathcal{M}}} dt_1 dt_2 \left( \frac{2t_2}{\pi} \right)^{\Delta_1 + \Delta_2 - 2} \left( \frac{2t_1}{\pi} \right)^{\Delta_3 + \Delta_4 - 2} (\Delta_3 - 1) A^m \left( \frac{A_1^g}{t_1} + A_2^g \right), \quad (3.43)$$

where we have defined the following matter and ghost correlators,

$$A^m \equiv \langle V_1(r_1) V_2(r_2) V_3(r_3) V_4(r_4) \rangle_{c_\ell}, \quad (3.44)$$

$$A_1^g \equiv \langle c(r_1) \mathcal{B}c(r_2) c(r_3) c(r_4) \rangle_{c_\ell}, \quad (3.45)$$

$$A_2^g \equiv \langle c(r_1) \mathcal{B}c(r_2) \partial c c(r_3) \mathcal{B}c(r_4) \rangle_{c_\ell}. \quad (3.46)$$

Here the insertion points and the circumference of the cylinder are given by

$$r_1 = \frac{1}{2}, \quad r_2 = \frac{1}{2} + t_2, \quad r_3 = \frac{3}{2} + t_2, \quad r_4 = \frac{3}{2} + t_2 + t_1, \quad l = t_1 + t_2 + 2. \quad (3.47)$$

As before, the evaluation of the ghost correlators is simplified by using cyclicity and the periodic identification to write

$$A_1^g = \langle \mathcal{B}c(r_2) c(r_3) c(r_4) c(r_1 + l) \rangle_{c_\ell}, \quad (3.48)$$

$$A_2^g = \langle \mathcal{B}c(r_2) \partial c c(r_3) \mathcal{B}c(r_4) c(r_1 + l) \rangle_{c_\ell}. \quad (3.49)$$

It is convenient to introduce the shorthand

$$\gamma \equiv \frac{\pi}{\ell} = \frac{\pi}{2 + t_1 + t_2}. \quad (3.50)$$

Using the formulas of appendix B, a calculation gives

$$\begin{aligned}
A_1^g &= -\frac{1}{\pi\gamma^2} \sin(\gamma) \sin(\gamma(t_1 + 1)) [(t_1 + 2) \sin(\gamma t_1) - t_1 \sin(\gamma(t_1 + 2))] , \\
A_2^g &= \frac{1}{\pi\gamma^2} \sin(\gamma) \sin(\gamma(t_1 + 1)) (\sin(\gamma t_1) - \sin(\gamma t_2)) \\
&\quad + \frac{1}{\pi\gamma} [\sin^2(\gamma) - \sin^2(\gamma t_1) + \sin^2(\gamma(t_1 + 1))] .
\end{aligned} \tag{3.51}$$

Combining terms we find

$$\frac{A_1^g}{t_1} + A_2^g = \frac{1}{\pi\gamma} (\cos(\gamma t_1) + \cos(\gamma t_2)) \left( \cos(\gamma t_1) - \frac{\sin(\gamma t_1)}{\gamma t_1} \right) . \tag{3.52}$$

An entirely analogous calculation gives

$$\mathcal{F}^{(2')} = - \int_{\widehat{\mathcal{M}}} dt_1 dt_2 \left( \frac{2t_2}{\pi} \right)^{\Delta_1 + \Delta_2 - 2} \left( \frac{2t_1}{\pi} \right)^{\Delta_3 + \Delta_4 - 2} (\Delta_4 - 1) A^m \left( \frac{A_1^g}{t_1} + A_3^g \right) , \tag{3.53}$$

where  $A_3^g \equiv \langle c(r_1) \mathcal{B} c(r_2) c(r_3) \mathcal{B} \partial c c(r_4) \rangle_{c_\ell}$ . Explicit computation reveals that  $A_3^g = A_2^g$ , so that

$$\mathcal{F}^{(2)} + \mathcal{F}^{(2')} = - \int_{\widehat{\mathcal{M}}} dt_1 dt_2 \left( \frac{2t_2}{\pi} \right)^{\Delta_1 + \Delta_2 - 2} \left( \frac{2t_1}{\pi} \right)^{\Delta_3 + \Delta_4 - 2} (\Delta_3 + \Delta_4 - 2) A^m \left( \frac{A_1^g}{t_1} + A_2^g \right) . \tag{3.54}$$

We now specialize to the case of tachyons  $V_i = e^{\alpha' p_i X}$ . Evaluating the matter correlator through (B.41) and collecting all the terms we finally find

$$\begin{aligned}
\mathcal{F}^{(2)} + \mathcal{F}^{(2')} &= - (2\pi)^D \delta \left( \sum p \right) \frac{1}{\pi} \left( \frac{2}{\pi} \right)^{\alpha' \sum p^2 - 4} (\alpha' (p_3^2 + p_4^2) - 2) \\
&\quad \cdot \int_{\widehat{\mathcal{M}}} dt_1 dt_2 \gamma^3 (\gamma t_2)^{\alpha' (p_1^2 + p_2^2) - 2} (\gamma t_1)^{\alpha' (p_3^2 + p_4^2) - 2} \\
&\quad \cdot (\cos(\gamma t_2) + \cos(\gamma t_1)) \left( \cos(\gamma t_1) - \frac{\sin(\gamma t_1)}{\gamma t_1} \right) \\
&\quad \cdot |\sin(\gamma t_1)|^{-\alpha' (s + p_3^2 + p_4^2)} \cdot |\sin(\gamma t_2)|^{-\alpha' (s + p_1^2 + p_2^2)} \\
&\quad \cdot |\sin \gamma|^{-\alpha' (2t + \sum p^2)} \cdot |\sin(\gamma(t_1 + 1))|^{\alpha' (2s + 2t + \sum p^2)} .
\end{aligned} \tag{3.55}$$

This is in agreement (up to an overall minus sign) with the result quoted in [32], as can be checked using the change of variables

$$T_1^{there} = \frac{2t_2}{t_1 + t_2 - 1} , \quad T_2^{there} = \frac{2t_1}{t_1 + t_2 - 1} . \tag{3.56}$$

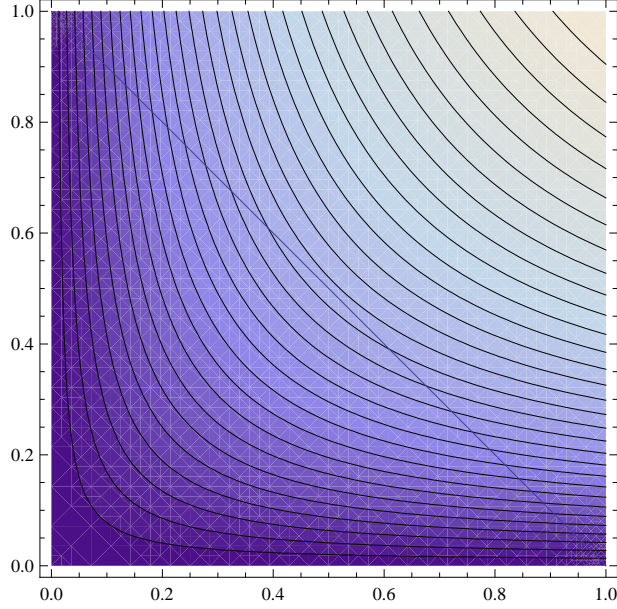


Figure 8: Curves of constant modulus  $\lambda$  on the  $t_1, t_2$  unit square. The triangle above the diagonal is the region of integration  $\widehat{\mathcal{M}}$  for the second string diagram (see Figure 6).

To understand the result we express it in terms of the modular parameter  $\lambda$  for the string diagram. Using (3.20) we find

$$\lambda = \frac{\sin(\gamma t_1) \sin(\gamma t_2)}{\sin^2(\gamma(t_1 + 1))}. \quad (3.57)$$

A small computation then gives

$$1 - \lambda = \frac{\sin^2(\gamma)}{\sin^2(\gamma(t_1 + 1))}. \quad (3.58)$$

It is interesting now to appreciate how  $\lambda$  varies as a function of  $t_1$  and  $t_2$ . Figure 8 shows the curves of constant  $\lambda$  on the unit square  $0 \leq t_1, t_2 \leq 1$ . Shown is also the diagonal that defines the upper right triangle as the relevant region of integration  $\widehat{\mathcal{M}}$ . The curves of  $\lambda = 0$  are the lines  $t_2 = 0$  and  $t_1 = 0$ . The point  $t_1 = t_2 = 1/2$  corresponds to  $\lambda = 1/4$ , so in fact, all curves of constant  $\lambda < 1/4$  intersect the diagonal twice. The curves with  $\lambda > 1/4$  are above the diagonal, and the point  $t_1 = t_2 = 1$  corresponds to  $\lambda = 1/2$ .

Using the modulus  $\lambda$  we can rewrite the amplitude as

$$\begin{aligned}
\mathcal{F}^{(2)} + \mathcal{F}^{(2')} &= (2\pi)^D \delta\left(\sum p\right) \frac{1}{\pi} \chi_{34} \\
&\cdot \int_{\widehat{\mathcal{M}}} dt_1 dt_2 \lambda^{-\alpha's-2} (1-\lambda)^{-\alpha't-2} \\
&\cdot \gamma^3 \frac{(\cos \gamma t_2 + \cos \gamma t_1)}{\sin^4 \gamma(t_1 + 1)} \left( \cos \gamma t_1 - \frac{\sin \gamma t_1}{\gamma t_1} \right) \\
&\cdot \left| \frac{\sin \gamma t_2}{\gamma t_2} \right|^{\chi_{12}} \cdot \left| \frac{\sin \gamma t_1}{\gamma t_1} \right|^{\chi_{34}} \cdot \left( \frac{\pi}{2} (1-\lambda)^{1/2} \right)^\chi.
\end{aligned} \tag{3.59}$$

To simplify the answer further we introduce the variable  $u$ :

$$u = \frac{\sin \gamma t_1}{\gamma t_1}. \tag{3.60}$$

The motivation for introducing  $u$  is that its derivative with respect to  $\gamma t_1$  produces the factor  $\cos \gamma t_1 - \frac{\sin \gamma t_1}{\gamma t_1}$ . Remarkably the full Jacobian gives

$$d\lambda \frac{du}{u} = \frac{1}{\pi} dt_1 dt_2 \frac{(\cos \gamma t_2 + \cos \gamma t_1)}{\sin^4 \gamma(t_1 + 1)} \left( \frac{\sin \gamma t_1}{\gamma t_1} - \cos \gamma t_1 \right). \tag{3.61}$$

The amplitude then collapses to a relatively simple form:

$$\begin{aligned}
\mathcal{F}^{(2)} + \mathcal{F}^{(2')} &= - (2\pi)^D \delta\left(\sum p\right) \int d\lambda du \lambda^{-\alpha's-2} (1-\lambda)^{-\alpha't-2} \\
&\cdot \left( \frac{\pi}{2} (1-\lambda)^{1/2} \right)^\chi \cdot \left| \frac{\sin \gamma t_2}{\gamma t_2} \right|^{\chi_{12}} \cdot \left( \frac{d}{du} u^{\chi_{34}} \right).
\end{aligned} \tag{3.62}$$

The region of integration here includes  $0 \leq \lambda \leq 1/2$  and values of  $u$  that depend on  $\lambda$  – the details of which have been anticipated in our discussion of Figure 8. Indeed,  $u$  is a parameter for the curves of constant modulus, and the integration is restricted over the upper right triangle. For  $0 \leq \lambda \leq 1/4$  each curve of constant modulus has two pieces inside the integration domain and one piece outside of it. For  $1/4 \leq \lambda \leq 1/2$  the curves of constant modulus are entirely contained inside the integration domain.

The diagram studied in this subsection (the second diagram) does not contribute to the pole at  $\alpha's + 1$ , it is a regular function at this kinematic point. To see this, it is easiest to start with the representation (3.55). Any singularity must arise because the integrand goes to infinity somewhere over the compact domain of integration. A little thought shows that this



can only happen at the corners where either  $t_1$  or  $t_2$  are equal to zero. In fact, when  $t_1$  is equal to zero the integrand is regular for  $\alpha's + 1 = 0$ . As  $t_2 \rightarrow 0$  there is a candidate singularity. To explore it, we make the change of variables  $(t_1, t_2) \rightarrow (\rho, t_2)$ , where

$$\rho \equiv \frac{t_1 - 1}{t_2}. \quad (3.63)$$

We then have

$$\int_{\widehat{\mathcal{M}}} dt_1 dt_2 = \int_0^1 d\rho \int_0^1 dt_2 t_2. \quad (3.64)$$

The extra factor of  $t_2$ , arising from the Jacobian, makes the integrand a finite function as  $t_2 \rightarrow 0$  and this establishes our claim. While there is no pole for  $\alpha's = -1$ , the amplitude under consideration has a pole for  $\alpha's = 0$ , corresponding to the exchange of on-shell massless states. There are also poles at positive integer values of  $\alpha's$ .

The failure of (3.62) to contribute to the pole at  $\alpha's + 1 = 0$  means that near that pole the full amplitude obtained from the first and second diagrams still behaves as in (3.31). We conclude that the full amplitude computed so far does not have the expected symmetry under the exchange  $(p_1, p_2) \leftrightarrow (p_3, p_4)$ .

## 4 Boundary term and exchange symmetry

The calculation of the previous section has failed to give a result consistent with the expected symmetry  $(p_1, p_2) \leftrightarrow (p_3, p_4)$ . The error can be traced to the naive manipulation (3.2), where a boundary term was inadvertently dropped. Let us repeat this manipulation more carefully. We introduce a regulated version of the propagator:

$$\mathcal{P}_{\Lambda\Lambda^*} \equiv \frac{B}{L_\Lambda} Q \frac{B^*}{L_{\Lambda^*}^*}, \quad (4.1)$$

where

$$\frac{1}{L_\Lambda} \equiv \int_0^\Lambda dT_1 e^{-T_1 L}, \quad \frac{1}{L_{\Lambda^*}^*} \equiv \int_0^{\Lambda^*} dT_2 e^{-T_2 L^*}. \quad (4.2)$$

Ultimately we are interested in taking the limit  $\Lambda, \Lambda^* \rightarrow \infty$ . Under BPZ conjugation the cutoffs  $\Lambda$  and  $\Lambda^*$  get interchanged,

$$\mathcal{P}_{\Lambda\Lambda^*}^* = \mathcal{P}_{\Lambda^*\Lambda}. \quad (4.3)$$

Using  $\{Q, B^*\} = L^*$ , we have

$$\mathcal{P}_{\Lambda\Lambda^*} = - \int_0^\Lambda dT_1 \int_0^{\Lambda^*} dT_2 B e^{-T_1 L} B^* e^{-T_2 L^*} Q + \int_0^\Lambda dT_1 \int_0^{\Lambda^*} dT_2 B e^{-T_1 L} \left( -\frac{d}{dT_2} e^{-T_2 L^*} \right), \quad (4.4)$$

which yields

$$\mathcal{P}_{\Lambda\Lambda^*} = -\frac{B}{L_\Lambda} \frac{B^*}{L_{\Lambda^*}} Q + \frac{B}{L_\Lambda} - \frac{B}{L_\Lambda} e^{-\Lambda^* L^*}. \quad (4.5)$$

The last term is the boundary term that was previously dropped. It gives an additional contribution to the four point function:

$$\mathcal{F}_{\Lambda\Lambda^*}^B \equiv -\left\langle \Psi_1 * \Psi_2, \int_0^\Lambda dT_1 B e^{-T_1 L} e^{-\Lambda^* L^*} (\Psi_3 * \Psi_4) \right\rangle. \quad (4.6)$$

It is useful to understand intuitively why the boundary term  $\frac{B}{L_\Lambda} e^{-\Lambda^* L^*}$  can give a contribution. Naively one would argue that in the limit  $\Lambda^* \rightarrow \infty$ , the factor  $e^{-\Lambda^* L^*}$  gives rise to degenerate Riemann surfaces and no regular contribution to amplitudes. It is the interplay with  $\frac{B}{L_\Lambda}$  that invalidates this argument. While  $e^{-\Lambda^* L^*}$  expands the surface by a scale factor of order  $e^{\Lambda^*}$ , the factor  $\frac{B}{L_\Lambda}$  sums over all surfaces obtained by contraction with scales that go from one down to about  $e^{-\Lambda}$ . If one takes the  $\Lambda \rightarrow \infty$  limit first, we have  $\frac{B}{L} e^{-\Lambda^* L^*}$ , which induces a very large expansion followed by a set of contractions that go down to zero size. This is a large set of *non-degenerate* surfaces. Had we taken the limit  $\Lambda^* \rightarrow 0$  first we would have indeed found only degenerate surfaces.

The terms previously computed,  $\mathcal{F}^{(1)}$  and  $\mathcal{F}^{(2)} + \mathcal{F}^{(2')}$ , do not depend on the precise way one takes  $\Lambda$  and  $\Lambda^*$  to infinity, in particular the order of the  $\Lambda$  and  $\Lambda^*$  limits can be safely interchanged. This is obvious for the first diagram, and is also true for the second diagram, because the integration region  $\widehat{\mathcal{M}}$  has an unambiguous limiting shape for large  $\Lambda$  and  $\Lambda^*$ . We define  $\mathcal{F}^B$  as a suitable limit of  $\mathcal{F}_{\Lambda\Lambda^*}^B$ . As anticipated above, we shall see that  $\mathcal{F}^B$  depends on the prescription used to take this limit. We choose the prescription by requiring that

- (i)  $\mathcal{F}^B$  vanishes for external on-shell states;
- (ii) the total amplitude  $\mathcal{F}_s = \mathcal{F}^{(1)} + \mathcal{F}^{(2)} + \mathcal{F}^{(2')} + \mathcal{F}^B$  is symmetric under  $(p_1, p_2) \leftrightarrow (p_3, p_4)$ .

Property (i) is necessary since for on-shell tachyons the naive calculation already gave the right result. We claim that the correct prescription is

$$\mathcal{P} \equiv \frac{1}{2} \left( \lim_{\Lambda \rightarrow \infty} \lim_{\Lambda^* \rightarrow \infty} + \lim_{\Lambda^* \rightarrow \infty} \lim_{\Lambda \rightarrow \infty} \right) \mathcal{P}_{\Lambda\Lambda^*}, \quad \mathcal{P}_{\Lambda\Lambda^*} = \frac{B}{L_\Lambda} Q \frac{B^*}{L_{\Lambda^*}}, \quad (4.7)$$

Using (4.3) we see that this leads to a BPZ even propagator, so barring calculational errors this prescription must give a four-point amplitude that obeys property (ii). We confirm this fact in the rest of the section: the exchange symmetry is restored by the boundary term (4.6) with the limits taken according to (4.7). Less obviously, property (i) also holds. It is non-trivial that a prescription with the right properties exists. We also re-examine work of §2.1 and confirm that

the propagator  $\mathcal{P}$  defined above provides an inverse to the kinetic operator in some appropriate sense.

## 4.1 Boundary term

We now turn to an explicit evaluation of the boundary term. By the techniques of §2, we find

$$\mathcal{F}_{\Lambda\Lambda^*}^B = - \int_{\frac{1}{s}}^1 \frac{dt}{t} \left\langle \Psi_1 * \Psi_2, B \left( W_{\frac{ts^*}{2}-t+\frac{1}{2}} * [\Psi_3]_{ts^*} * [\Psi_4]_{ts^*} * W_{\frac{ts^*}{2}-t+\frac{1}{2}} \right) \right\rangle, \quad (4.8)$$

where we have set

$$s \equiv e^\Lambda, \quad s^* \equiv e^{\Lambda^*}. \quad (4.9)$$

We evaluate the action of  $B$ , assuming that  $\Psi_3$  and  $\Psi_4$  are in Schnabl gauge:

$$\begin{aligned} & B \left( W_{\frac{ts^*}{2}-t+\frac{1}{2}} * [\Psi_3]_{ts^*} * [\Psi_4]_{ts^*} * W_{\frac{ts^*}{2}-t+\frac{1}{2}} \right) = \\ & t(1-s^*) W_{\frac{ts^*}{2}-t+\frac{1}{2}} * B_L^+ [\Psi_3]_{ts^*} * [\Psi_4]_{ts^*} * W_{\frac{ts^*}{2}-t+\frac{1}{2}} \\ & - ts^* (-1)^{\Psi_3} W_{\frac{ts^*}{2}-t+\frac{1}{2}} * [\Psi_3]_{ts^*} * B_L^+ [\Psi_4]_{ts^*} * W_{\frac{ts^*}{2}-t+\frac{1}{2}} \\ & + t(1-s^*) (-1)^{\Psi_3+\Psi_4} W_{\frac{ts^*}{2}-t+\frac{1}{2}} * [\Psi_3]_{ts^*} * [\Psi_4]_{ts^*} * B_L^+ W_{\frac{ts^*}{2}-t+\frac{1}{2}}. \end{aligned} \quad (4.10)$$

Back in (4.8) and changing the integration variable to  $x = s^*t$ ,

$$\begin{aligned} \mathcal{F}_{\Lambda\Lambda^*}^B = \int_{\frac{s^*}{s}}^{s^*} dx \left\{ \right. & \left(1 - \frac{1}{s^*}\right) \langle \Psi_1 * \Psi_2, W_{\frac{x}{2}-\frac{x}{s^*}+\frac{1}{2}} * B_L^+ [\Psi_3]_x * [\Psi_4]_x * W_{\frac{x}{2}-\frac{x}{s^*}+\frac{1}{2}} \rangle \\ & + (-1)^{\Psi_3} \langle \Psi_1 * \Psi_2, W_{\frac{x}{2}-\frac{x}{s^*}+\frac{1}{2}} * [\Psi_3]_x * B_L^+ [\Psi_4]_x * W_{\frac{x}{2}-\frac{x}{s^*}+\frac{1}{2}} \rangle \\ & \left. + (-1)^{\Psi_3+\Psi_4} \left(1 - \frac{1}{s^*}\right) \langle \Psi_1 * \Psi_2, W_{\frac{x}{2}-\frac{x}{s^*}+\frac{1}{2}} * [\Psi_3]_x * [\Psi_4]_x * B_L^+ W_{\frac{x}{2}-\frac{x}{s^*}+\frac{1}{2}} \rangle \right\}. \end{aligned} \quad (4.11)$$

We now remove the regulators using the symmetrized prescription (4.7). The first term in (4.7) is an instruction to send  $s^* \rightarrow \infty$  first: then both the lower and upper limits of integration in (4.11) go to infinity, and only the singular surface with  $x = \infty$  is kept. We believe that this singular surface gives no contribution to the integral – the first term in (4.7) does not contribute to  $\mathcal{F}^B$ . On the other hand, the second term in (4.7) gives a regular contribution:

$$\begin{aligned} \mathcal{F}^B = \frac{1}{2} \int_0^\infty dx \left\{ \right. & \left\langle \Psi_1 * \Psi_2, W_{\frac{x}{2}+\frac{1}{2}} * B_L^+ [\Psi_3]_x * [\Psi_4]_x * W_{\frac{x}{2}+\frac{1}{2}} \right\rangle \\ & + (-1)^{\Psi_3} \left\langle \Psi_1 * \Psi_2, W_{\frac{x}{2}+\frac{1}{2}} * [\Psi_3]_x * B_L^+ [\Psi_4]_x * W_{\frac{x}{2}+\frac{1}{2}} \right\rangle \\ & \left. + (-1)^{\Psi_3+\Psi_4} \left\langle \Psi_1 * \Psi_2, W_{\frac{x}{2}+\frac{1}{2}} * [\Psi_3]_x * [\Psi_4]_x * B_L^+ W_{\frac{x}{2}+\frac{1}{2}} \right\rangle \right\}. \end{aligned} \quad (4.12)$$

The first term in this amplitude is illustrated in the string diagram of Figure 9. Restricting to

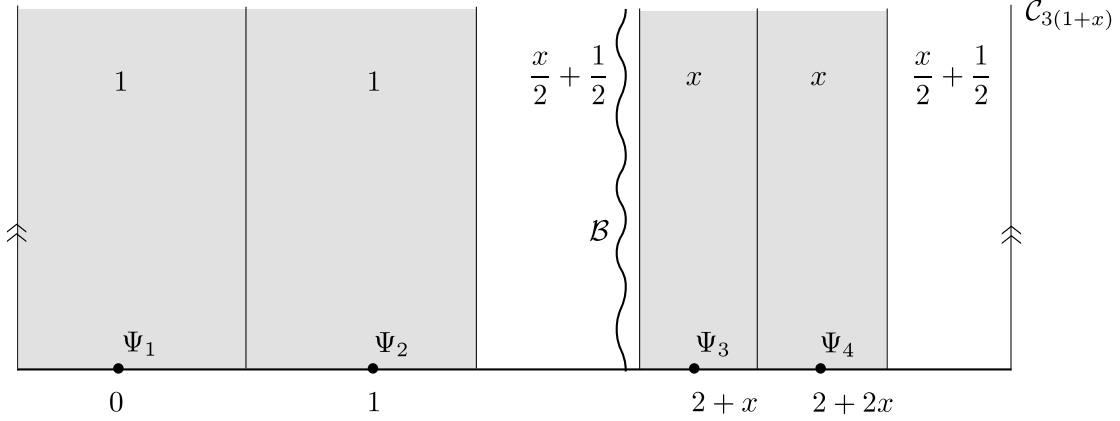


Figure 9: The string diagram for the first term in the boundary amplitude  $\mathcal{F}^B$  in (4.12).

the case of tachyons, we find

$$\mathcal{F}^B = \frac{1}{2} \int_0^\infty dx \left( \frac{2}{\pi} \right)^{\alpha' \sum p_i^2 - 4} x^{\alpha' (p_3^2 + p_4^2) - 2} A^g A^m, \quad (4.13)$$

where the matter and ghost correlators are defined by

$$A^m = \langle e^{ip_1 \cdot X(r_1)} e^{ip_2 \cdot X(r_2)} e^{ip_3 \cdot X(r_3)} e^{ip_4 \cdot X(r_4)} \rangle_{c_\ell} \quad (4.14)$$

$$A^g = -\langle c(r_1)c(r_2)\mathcal{B}c(r_3)c(r_4) \rangle_{c_\ell} + \langle c(r_1)c(r_2)c(r_3)\mathcal{B}c(r_4) \rangle_{c_\ell} - \langle c(r_1)c(r_2)c(r_3)c(r_4)\mathcal{B} \rangle_{c_\ell}.$$

Here the insertion points and circumference of the cylinder are

$$r_1 = 0, \quad r_2 = 1, \quad r_3 = 2 + x, \quad r_4 = 2 + 2x, \quad \ell = 3 + 3x. \quad (4.15)$$

We also define

$$\gamma' = \frac{\pi}{\ell} = \frac{\pi}{3} \frac{1}{1+x}. \quad (4.16)$$

The modular parameter for this geometry is

$$\lambda = \frac{\sin(\gamma') \sin(\gamma'x)}{\sin^2(\gamma'(x+2))}, \quad 1 - \lambda = \frac{3}{4} \frac{1}{\sin^2(\gamma'(x+2))}. \quad (4.17)$$

One readily finds that  $\lambda(1/x) = \lambda(x)$ . The modular region  $\lambda \in [0, \frac{1}{4}]$  is covered once as  $x$  goes from 0 to 1, and once again as  $x$  goes from 1 to  $\infty$ .

Using (B.41), the matter correlator is

$$\begin{aligned} A^m &= (2\pi)^D \delta \left( \sum p \right) \gamma'^{\alpha' \sum p_i^2} \\ &\cdot \sin(\gamma')^{-\alpha'(\mathbf{s} + p_1^2 + p_2^2)} \cdot \sin(\gamma'x)^{-\alpha'(\mathbf{s} + p_3^2 + p_4^2)} \\ &\cdot \sin(\gamma'(2+x))^{\alpha'(2\mathbf{s} + 2\mathbf{t} + \sum p_i^2)} (\sqrt{3}/2)^{-\alpha'(2\mathbf{t} + \sum p_i^2)} \end{aligned} \quad (4.18)$$

From (B.39) we find the ghost correlator

$$A^g = -\frac{81}{4\pi^3}(1+x)^2 \sin \gamma'(1-x). \quad (4.19)$$

Assembling partial results,

$$\begin{aligned} \mathcal{F}^B = & -(2\pi)^D \delta \left( \sum p \right) \left( \frac{2}{\pi} \right)^{\alpha' \sum p_i^2 - 4} \int_0^\infty dx \frac{\pi}{8} \frac{1}{(1+x)^2} \frac{\sin \gamma'(1-x)}{\sin^4(\gamma'(2+x))} \\ & \cdot \lambda^{-\alpha' s - 2} (1-\lambda)^{-\alpha' t - 2} \left( \frac{2}{\sqrt{3}} \sin(\gamma'(2+x)) \right)^{-4 + \alpha' \sum p^2} \cdot \left( \frac{\sin \gamma'}{\gamma'} \right)^{\chi_{12}} \left( \frac{\sin \gamma' x}{\gamma' x} \right)^{\chi_{34}}. \end{aligned} \quad (4.20)$$

Under the change of variables  $x \rightarrow 1/x$ , the integral (4.20) goes into minus the same expression with  $\chi_{12} \leftrightarrow \chi_{34}$ . Thus we can restrict the integration region to  $x \in [0, 1]$ , provided we antisymmetrize the integrand under the exchange  $\chi_{12} \leftrightarrow \chi_{34}$ :

$$\begin{aligned} \mathcal{F}^B = & -(2\pi)^D \delta \left( \sum p \right) \left( \frac{2}{\pi} \right)^{\alpha' \sum p_i^2 - 4} \int_0^1 dx \frac{\pi}{8} \frac{1}{(1+x)^2} \frac{\sin \gamma'(1-x)}{\sin^4(\gamma'(2+x))} \\ & \cdot \lambda^{-\alpha' s - 2} (1-\lambda)^{-\alpha' t - 2} \left( \frac{2}{\sqrt{3}} \sin(\gamma'(2+x)) \right)^{-x} \\ & \cdot \left[ \left( \frac{\sin \gamma'}{\gamma'} \right)^{\chi_{12}} \left( \frac{\sin \gamma' x}{\gamma' x} \right)^{\chi_{34}} - \left( \frac{\sin \gamma' x}{\gamma' x} \right)^{\chi_{12}} \left( \frac{\sin \gamma'}{\gamma'} \right)^{\chi_{34}} \right]. \end{aligned} \quad (4.21)$$

To change variables of integration from  $x$  to  $\lambda$  we use

$$d\lambda = \frac{\pi}{4} \frac{dx}{(1+x)^2} \frac{\sin \gamma'(1-x)}{\sin^4(\gamma'(2+x))}. \quad (4.22)$$

The amplitude then becomes

$$\begin{aligned} \mathcal{F}^B = & -(2\pi)^D \delta \left( \sum p \right) \int_0^{1/4} d\lambda \lambda^{-\alpha' s - 2} (1-\lambda)^{-\alpha' t - 2} \cdot \left( \frac{\pi}{2} (1-\lambda)^{1/2} \right)^x \\ & \cdot \frac{1}{2} \left[ \left( \frac{\sin \gamma'}{\gamma'} \right)^{\chi_{12}} \left( \frac{\sin \gamma' x}{\gamma' x} \right)^{\chi_{34}} - \left( \frac{\sin \gamma' x}{\gamma' x} \right)^{\chi_{12}} \left( \frac{\sin \gamma'}{\gamma'} \right)^{\chi_{34}} \right]. \end{aligned} \quad (4.23)$$

The boundary term is antisymmetric under the exchange symmetry,

$$\mathcal{F}^B \leftrightarrow -\mathcal{F}^B \quad \text{under} \quad (p_1, p_2) \leftrightarrow (p_3, p_4). \quad (4.24)$$

In particular, when the momenta are on-shell  $\chi_{12} = \chi_{34} = 0$  and  $\mathcal{F}^B = 0$ .

As a first check that the boundary term restores the exchange symmetry, let us extract the pole at  $\alpha's + 1 = 0$ , which arises for  $\lambda \sim 0$  or  $x \sim 0$ . As  $x \sim 0$ , we have  $\frac{\sin \gamma'}{\gamma'} \sim \frac{2}{\pi} \frac{3\sqrt{3}}{4}$  so we get:

$$\mathcal{F}^B|_{pole} \simeq (2\pi)^D \delta \left( \sum p \right) \left[ -\frac{1}{\alpha's + 1} \right] \cdot \frac{1}{2} \left[ -\left( \frac{3\sqrt{3}}{4} \right)^{\chi_{12}} \left( \frac{\pi}{2} \right)^{\chi_{34}} + \left( \frac{\pi}{2} \right)^{\chi_{12}} \left( \frac{3\sqrt{3}}{4} \right)^{\chi_{34}} \right]. \quad (4.25)$$

Combining this with (3.31), we find that for the full amplitude,

$$\mathcal{F}_s|_{pole} \simeq (2\pi)^D \delta \left( \sum p \right) \left[ -\frac{1}{\alpha's + 1} \right] \cdot \frac{1}{2} \left[ \left( \frac{3\sqrt{3}}{4} \right)^{\chi_{12}} \left( \frac{\pi}{2} \right)^{\chi_{34}} + \left( \frac{\pi}{2} \right)^{\chi_{12}} \left( \frac{3\sqrt{3}}{4} \right)^{\chi_{34}} \right]. \quad (4.26)$$

So the exchange symmetry holds near the pole. In the next subsection we prove that the symmetry is exactly obeyed for arbitrary values of the momenta.

Though symmetric, the amplitude near the pole does *not* factorize into the product of two off-shell vertices. A factorized answer would read

$$\mathcal{F}_s^{factor}|_{pole} \simeq (2\pi)^D \delta \left( \sum p \right) \left[ -\frac{1}{\alpha's + 1} \right] \cdot \left( \frac{3\sqrt{3}}{4} \right)^{\chi_{12}} \left( \frac{3\sqrt{3}}{4} \right)^{\chi_{34}}. \quad (4.27)$$

Indeed, the coefficient  $(3\sqrt{3}/4)^{\alpha' p_i^2 - 1}$  is the conformal factor that arises in inserting a tachyon vertex operator on the Witten vertex. Factorization holds in Siegel gauge, where it has a transparent geometric interpretation. The Siegel gauge propagator is a strip of canonical width  $\pi$  and length equal to the Schwinger parameter  $T$ . The pole arises for  $T \rightarrow \infty$ ; where the string diagram manifestly splits into two off-shell vertices attached to each side of a long propagator. By contrast, the geometric interpretation of the Schnabl propagator does not suggest off-shell factorization.

A natural question is whether the prescription (4.7) is unique. There are other ways to achieve a BPZ symmetric propagator, perhaps the simplest being

$$\mathcal{P} \stackrel{?}{=} \lim_{\Lambda \rightarrow \infty} \mathcal{P}_{\Lambda\Lambda}. \quad (4.28)$$

Using this prescription, the  $x$  integration in (4.11) would range from 1 to  $\infty$ . Performing the same steps as above, we would arrive at the boundary term

$$\begin{aligned} \tilde{\mathcal{F}}^B = & -(2\pi)^D \delta \left( \sum p \right) \int_0^{1/4} d\lambda \lambda^{-\alpha's-2} (1-\lambda)^{-\alpha't-2} \cdot \left( \frac{\pi}{2} (1-\lambda)^{1/2} \right)^x \\ & \cdot \left[ -\left( \frac{\sin \gamma' x}{\gamma' x} \right)^{\chi_{12}} \left( \frac{\sin \gamma'}{\gamma'} \right)^{\chi_{34}} \right]. \end{aligned} \quad (4.29)$$

The difference  $\tilde{\mathcal{F}}^B - \mathcal{F}^B$  is symmetric under  $\chi_{12} \leftrightarrow \chi_{34}$ . It follows that the total amplitude  $\tilde{\mathcal{F}}_s$  computed with the prescription (4.28) is symmetric just like the total amplitude  $\mathcal{F}_s$  computed

with the prescription (4.7). However,  $\widetilde{\mathcal{F}}_{\mathbf{s}}$  does not agree on shell with the standard Veneziano formula, since the boundary term (4.29) does not vanish on-shell. As we will discuss in §4.3, (4.28) does not really invert the kinetic operator  $\mathcal{K}$  discussed in §2.1 while (4.7) does. It appears that (4.7) is the only prescription leading to a four-point amplitude that is correct on-shell and has the right exchange symmetry.

## 4.2 Proof of exchange symmetry

Our final result for the off-shell Veneziano amplitude is

$$\mathcal{F}_{\mathbf{s}} = \mathcal{F}^{(1)} + \mathcal{F}^{(2)} + \mathcal{F}^{(2')} + \mathcal{F}^B, \quad (4.30)$$

where  $\mathcal{F}^{(1)}$ ,  $\mathcal{F}^{(2)} + \mathcal{F}^{(2')}$ , and  $\mathcal{F}^B$  are given in (3.29), (3.62) and (4.23), respectively. Collecting our results we have

$$\begin{aligned} \mathcal{F}_{\mathbf{s}} = & (2\pi)^D \delta(\sum p) \int_0^{\frac{1}{2}} d\lambda \lambda^{-\alpha' s - 2} (1 - \lambda)^{-\alpha' t - 2} \\ & \cdot \left[ \frac{\pi}{2} (1 - \lambda)^{1/2} \right]^x \left\{ \left[ \frac{3+t}{\pi} \sin \left[ \frac{\pi}{3+t} \right] \right]^x \left[ \frac{\lambda}{t(1-\lambda)} \right]^{\chi_{34}} - \int du \left| \frac{\sin \gamma t_2}{\gamma t_2} \right|^{\chi_{12}} \frac{du^{\chi_{34}}}{du} \right. \\ & \left. - \frac{1}{2} \theta \left( \frac{1}{4} - \lambda \right) \left( \left| \frac{\sin \gamma'}{\gamma'} \right|^{\chi_{12}} \left| \frac{\sin \gamma' x}{\gamma' x} \right|^{\chi_{34}} - \left| \frac{\sin \gamma'}{\gamma'} \right|^{\chi_{34}} \left| \frac{\sin \gamma' x}{\gamma' x} \right|^{\chi_{12}} \right) \right\}. \end{aligned} \quad (4.31)$$

Here  $\gamma = \pi/(2 + t_1 + t_2)$  and  $\gamma' = \pi/(3(1+x))$ . The function  $\theta(1/4 - \lambda)$  in the last term is the step-function  $\theta(\mu) = 0$  for  $\mu < 0$ ,  $\theta(\mu) = 1$  for  $\mu > 0$ , and it encodes the vanishing of the boundary integrand for  $\lambda > 1/4$ . The limits of integration for  $u$  are also  $\lambda$  dependent, as we will discuss shortly.

We now demonstrate that  $\mathcal{F}_{\mathbf{s}}$ , as given in (4.31), is symmetric under the exchange  $(p_1, p_2) \leftrightarrow (p_3, p_4)$ . Since  $\mathbf{s}$  and  $\mathbf{t}$  are invariant under this exchange and the momenta enter  $\mathcal{F}_{\mathbf{s}}$  only through  $\chi_{12}$  and  $\chi_{34}$ , we are effectively testing the symmetry of  $\mathcal{F}_{\mathbf{s}}$  under the exchange  $\chi_{12} \leftrightarrow \chi_{34}$ . We will show that the symmetry holds *locally* on moduli space, that is, before performing the  $\lambda$  integration. For this only the terms inside the braces  $\{ \dots \}$  need to be looked at.

The symmetry property would be established if

$$\begin{aligned} 0 = & \left[ \frac{\sin \left[ \frac{\pi}{3+t} \right]}{\frac{\pi}{3+t}} \right]^x \left( \left[ \frac{\lambda}{t(1-\lambda)} \right]^{\chi_{34}} - \left[ \frac{\lambda}{t(1-\lambda)} \right]^{\chi_{12}} \right) \\ & - \int du \left( \left| \frac{\sin \gamma t_2}{\gamma t_2} \right|^{\chi_{12}} \frac{du^{\chi_{34}}}{du} - \left| \frac{\sin \gamma t_2}{\gamma t_2} \right|^{\chi_{34}} \frac{du^{\chi_{12}}}{du} \right) \\ & - \theta \left( \frac{1}{4} - \lambda \right) \left( \left| \frac{\sin \gamma'}{\gamma'} \right|^{\chi_{12}} \left| \frac{\sin \gamma' x}{\gamma' x} \right|^{\chi_{34}} - \left| \frac{\sin \gamma'}{\gamma'} \right|^{\chi_{34}} \left| \frac{\sin \gamma' x}{\gamma' x} \right|^{\chi_{12}} \right). \end{aligned} \quad (4.32)$$

We begin by showing that the middle term is the integral of a total derivative. We recall the definition of  $u$  and introduce a companion variable  $v$ :

$$u(t_1, t_2) = \frac{\sin \gamma t_1}{\gamma t_1}, \quad v(t_1, t_2) = \frac{\sin \gamma t_2}{\gamma t_2}. \quad (4.33)$$

Consider one of the curves of constant  $\lambda$  in the  $t_1, t_2$  diagram (Figure 10). The curve is invariant under the reflection  $t_1 \leftrightarrow t_2$  and goes from  $u = u_i$  to  $u = u_f$ . Consider a parameterization of this curve with a parameter  $\sigma \in [0, 1]$ :

$$t_1 = t_1(\sigma), \quad t_2 = t_2(\sigma), \quad (4.34)$$

with the condition that the points at  $\sigma$  and at  $1 - \sigma$  are reflections of one another:

$$t_1(1 - \sigma) = t_2(\sigma), \quad t_2(1 - \sigma) = t_1(\sigma). \quad (4.35)$$

Through these relations we can now view  $u$  and  $v$ , on the constant  $\lambda$  curve as just functions of  $\sigma$ :  $u(\sigma), v(\sigma)$ . We demand that  $u(0) = u_i$  and  $u(1) = u_f$ . Given the parameterization and the fact that  $u \leftrightarrow v$  as  $t_1 \leftrightarrow t_2$ , we have

$$v(\sigma) = u(1 - \sigma). \quad (4.36)$$

The middle term in (4.32) is

$$\begin{aligned} & - \int_{u_i}^{u_f} d\sigma \left( v(\sigma)^{\chi_{12}} \frac{d}{d\sigma} u(\sigma)^{\chi_{34}} - v(\sigma)^{\chi_{34}} \frac{d}{d\sigma} u(\sigma)^{\chi_{12}} \right) \\ &= - \int_0^1 d\sigma \left( u(1 - \sigma)^{\chi_{12}} \frac{d}{d\sigma} u(\sigma)^{\chi_{34}} - u(1 - \sigma)^{\chi_{34}} \frac{d}{d\sigma} u(\sigma)^{\chi_{12}} \right) \\ &= - \int_0^1 d\sigma \left( u(1 - \sigma)^{\chi_{12}} \frac{d}{d\sigma} u(\sigma)^{\chi_{34}} + \frac{d}{d\sigma} u(1 - \sigma)^{\chi_{12}} u(\sigma)^{\chi_{34}} \right) \quad (4.37) \\ &= - \int_0^1 d\sigma \frac{d}{d\sigma} \left( u(1 - \sigma)^{\chi_{12}} u(\sigma)^{\chi_{34}} \right) \\ &= - \left( u(0)^{\chi_{12}} u(1)^{\chi_{34}} - u(1)^{\chi_{12}} u(0)^{\chi_{34}} \right) = u_f^{\chi_{12}} u_i^{\chi_{34}} - u_f^{\chi_{34}} u_i^{\chi_{12}}. \end{aligned}$$

In the last equality we assumed  $\lambda > 1/4$ , in which case the constant  $\lambda$  curves that do not intersect the diagonal and the integration region indeed goes from  $u_i$  to  $u_f$ . For  $\lambda < 1/4$  the integral is really of the form

$$- \int_{u_i}^{u_-} \dots - \int_{u_+}^{u_f} \dots = - \int_{u_i}^{u_f} \dots + \int_{u_-}^{u_+} \dots \quad (4.38)$$



where  $u_- < u_+$  are the points on the curve that are also on the diagonal  $t_1 + t_2 = 1$  (Figure 10). Therefore, for  $\lambda < 1/4$  we get the *extra* terms

$$-u_+^{\chi_{12}} u_-^{\chi_{34}} + u_+^{\chi_{34}} u_-^{\chi_{12}}. \quad (4.39)$$

It now follows that (4.32) holds if the following two identities are satisfied:

$$0 = \left[ \frac{\sin \left[ \frac{\pi}{3+t} \right]}{\frac{\pi}{3+t}} \right]^\chi \left( \left[ \frac{\lambda}{t(1-\lambda)} \right]^{\chi_{34}} - \left[ \frac{\lambda}{t(1-\lambda)} \right]^{\chi_{12}} \right) + u_f^{\chi_{12}} u_i^{\chi_{34}} - u_f^{\chi_{34}} u_i^{\chi_{12}} \quad (4.40)$$

$$0 = -u_+^{\chi_{12}} u_-^{\chi_{34}} + u_+^{\chi_{34}} u_-^{\chi_{12}} - \left( \left| \frac{\sin \gamma'}{\gamma'} \right|^{\chi_{12}} \left| \frac{\sin \gamma' x}{\gamma' x} \right|^{\chi_{34}} - \left| \frac{\sin \gamma'}{\gamma'} \right|^{\chi_{34}} \left| \frac{\sin \gamma' x}{\gamma' x} \right|^{\chi_{12}} \right). \quad (4.41)$$

The above identities are antisymmetric under the exchange  $\chi_{12} \leftrightarrow \chi_{34}$ . It is then sufficient to show that:

$$0 = \left[ \frac{\sin \left[ \frac{\pi}{3+t} \right]}{\frac{\pi}{3+t}} \right]^\chi \left[ \frac{\lambda}{t(1-\lambda)} \right]^{\chi_{34}} - u_f^{\chi_{34}} u_i^{\chi_{12}}, \quad (4.42)$$

$$0 = -u_+^{\chi_{12}} u_-^{\chi_{34}} + \left| \frac{\sin \gamma'}{\gamma'} \right|^{\chi_{34}} \left| \frac{\sin \gamma' x}{\gamma' x} \right|^{\chi_{12}}.$$

Consider the first relation. It follows from the modulus calculation in the first diagram that

$$\frac{\lambda}{t(1-\lambda)} = \frac{\sin \left[ \frac{\pi t}{3+t} \right]}{t \sin \left[ \frac{\pi}{3+t} \right]}. \quad (4.43)$$

Then

$$\left[ \frac{\sin \left[ \frac{\pi}{3+t} \right]}{\frac{\pi}{3+t}} \right]^\chi \left[ \frac{\lambda}{t(1-\lambda)} \right]^{\chi_{34}} = \left[ \frac{\sin \left[ \frac{\pi t}{3+t} \right]}{\frac{\pi t}{3+t}} \right]^{\chi_{34}} \left[ \frac{\sin \left[ \frac{\pi}{3+t} \right]}{\frac{\pi}{3+t}} \right]^{\chi_{12}}. \quad (4.44)$$

The second term on the first relation is associated with the second diagram. The point  $u_i$  corresponds to  $t_1 = 1$  and some value  $t_2 = \bar{t}$ . The point  $u_f$  corresponds to  $t_2 = 1$  and  $t_1 = \bar{t}$  (see Figure 10). Hence,

$$u_f = \frac{\sin \left[ \frac{\pi \bar{t}}{3+\bar{t}} \right]}{\frac{\pi \bar{t}}{3+\bar{t}}}, \quad u_i = \frac{\sin \left[ \frac{\pi}{3+t} \right]}{\frac{\pi}{3+t}}. \quad (4.45)$$

The modulus  $\lambda$  for the curve in question is given by (3.57), using  $t_1 = 1, t_2 = \bar{t}$ :

$$\lambda = \frac{\sin \left[ \frac{\pi}{3+t} \right] \sin \left[ \frac{\pi \bar{t}}{3+\bar{t}} \right]}{\sin^2 \left[ \frac{2\pi}{3+t} \right]}. \quad (4.46)$$

Comparing with (3.21) we see that for fixed  $\lambda$  we have  $\bar{t} = t$ . It then follows from (4.45) that  $u_f^{\chi_{34}} u_i^{\chi_{12}}$  coincides with the right hand side of (4.44). This proves the first equality in (4.42).

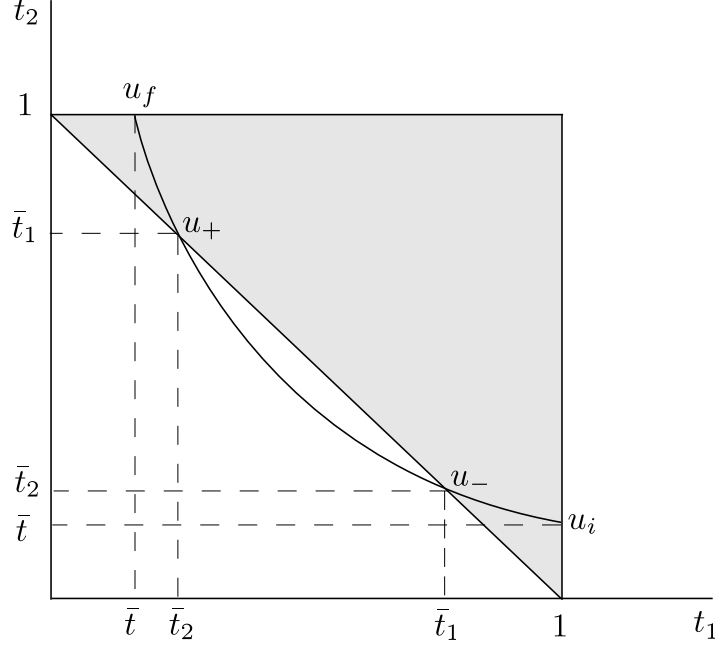


Figure 10: Auxiliary diagram for the proof of symmetry.

To prove the second relation in (4.42) we first note that  $u_-$  corresponds to  $t_1 + t_2 = 1$ , which gives  $\gamma = \pi/3$ , and some values  $\bar{t}_1$  and  $\bar{t}_2$  for  $t_1$  and  $t_2$ , such that  $\bar{t}_1 > 1/2$  (see Figure 10). The modulus associated with  $u_-$  (or  $u_+$ , since it lies on the same curve) is (3.58),

$$1 - \lambda = \frac{3}{4} \frac{1}{\sin^2(\frac{\pi}{3}(\bar{t}_1 + 1))}. \quad (4.47)$$

For the second term on the right-hand side of the equality the modulus is the function of  $x$  given by (4.17),

$$1 - \lambda = \frac{3}{4} \frac{1}{\sin^2[\frac{\pi(x+2)}{3(1+x)}]}. \quad (4.48)$$

It follows from the last two equations that

$$\bar{t}_1 = \frac{1}{1+x} \quad \rightarrow \quad \gamma' = \frac{\pi}{3} \frac{1}{1+x} = \gamma \bar{t}_1, \quad \gamma' x = \gamma \bar{t}_2. \quad (4.49)$$

Since  $0 < x < 1$ , we have  $\bar{t}_1 < 1/2$ , as required. Therefore:

$$\frac{\sin \gamma'}{\gamma'} = \frac{\sin \gamma \bar{t}_1}{\gamma \bar{t}_1} = u_-, \quad \text{and} \quad \frac{\sin \gamma' x}{\gamma' x} = \frac{\sin \gamma \bar{t}_2}{\gamma \bar{t}_2} = u_+. \quad (4.50)$$

These relations make it clear that the second equation in (4.42) also holds. This completes the proof that  $\mathcal{F}_s$  has the requisite exchange symmetry.

Having reassured ourselves that the symmetry holds, we can write a *manifestly* symmetric form of the amplitude by averaging over the two orderings 1234 and 3412,

$$\boxed{
\begin{aligned}
\mathcal{F}_s = & (2\pi)^D \delta(\sum p) \int_0^{\frac{1}{2}} d\lambda \lambda^{-\alpha's-2} (1-\lambda)^{-\alpha't-2} \cdot \left[ \frac{\pi}{2} (1-\lambda)^{1/2} \right]^\chi \\
& \left\{ \frac{1}{2} \left[ \frac{3+t}{\pi} \sin \left[ \frac{\pi}{3+t} \right] \right]^\chi \left( \left[ \frac{\lambda}{t(1-\lambda)} \right]^{\chi_{34}} + \left[ \frac{\lambda}{t(1-\lambda)} \right]^{\chi_{12}} \right) \right. \\
& \left. - \frac{1}{2} \int du \left( \left| \frac{\sin \gamma t_2}{\gamma t_2} \right|^{\chi_{12}} \frac{du^{\chi_{34}}}{du} + \left| \frac{\sin \gamma t_2}{\gamma t_2} \right|^{\chi_{34}} \frac{du^{\chi_{12}}}{du} \right) \right\}.
\end{aligned}
} \tag{4.51}$$

This is the final and most useful form of  $\mathcal{F}_s$ . For ease of reference, we recall that the variable  $t$  is a function of the modulus  $\lambda$ , given by (3.22); the variable  $t_2$  should be thought as a function of  $\lambda$  and of the integration variable  $u$ , according to the definitions given in (3.57) and (3.60); the variables  $\chi$ ,  $\chi_{12}$  and  $\chi_{34}$  are functions of the external momenta, given in (3.28). The limits of integration for  $u$  are from  $u_i$  to  $u_f$  for  $1/4 \leq \lambda \leq 1/2$  and from  $u_i$  to  $u_-$  together with  $u_+$  to  $u_f$ , for  $0 \leq \lambda \leq 1/4$ .

Our computation has given us the full **s**-channel contribution  $\mathcal{F}_s$  to the amplitude when the punctures appear as 1234 as we travel on the boundary of the circle in the counterclockwise direction. We can rewrite (4.51) as

$$\mathcal{F}_s = (2\pi)^D \delta(\sum p) \int_0^{\frac{1}{2}} d\lambda \lambda^{-\alpha's-2} (1-\lambda)^{-\alpha't-2} F(\lambda, \chi_{ij}), \tag{4.52}$$

where introduced the function  $F$  of the modulus  $\lambda$  and of the  $\chi_{ij}$  invariants. As we discussed at the end of §3.1, the **t**-channel contribution would be given by

$$\mathcal{F}_t = (2\pi)^D \delta(\sum p) \int_{1/2}^1 d\lambda \lambda^{-\alpha's-2} (1-\lambda)^{-\alpha't-2} F(1-\lambda, \chi_{i+1, j+1}). \tag{4.53}$$

The off-shell continuity of the integrand for combined **s**- and **t**-channel amplitudes requires  $F(1/2, \chi_{ij}) = F(1/2, \chi_{i+1, j+1})$ . This holds on account of our earlier analysis, since neither the second diagram nor the third one contribute for  $\lambda = 1/2$ . The off-shell Veneziano amplitude  $A(\mathbf{s}, \mathbf{t})$  is given by

$$A(\mathbf{s}, \mathbf{t}) = \mathcal{F}_s + \mathcal{F}_t. \tag{4.54}$$

The full four-tachyon amplitude is obtained by adding to  $A(\mathbf{s}, \mathbf{t})$  the other terms that correspond to in-equivalent orderings of four punctures on the boundary of a disk.

### 4.3 The propagator revisited

We have defined a propagator  $\mathcal{P}$  in (4.7) that leads to a sensible off-shell amplitude for four tachyons. It is natural now to revisit the formal computations of §2.1 to see if this propagator, with its regulation and symmetrized limits, provides an inverse to the kinetic operator on the gauge slice. We ask if the propagator  $\mathcal{P}$  really satisfies  $\mathcal{P}\mathcal{K} = P$  where, as before,  $P = BC$  is the projector to the gauge slice. As it turns out this equation is *not* satisfied. What we will find is that, with our definition,

$$\mathcal{P}\mathcal{K} = P + Q\eta. \quad (4.55)$$

In the above operator equation we find  $BQ\eta = 0$  and  $B\eta = 0$ . Acting on arbitrary states, the extra term on the right-hand side is therefore a truly trivial state in the gauge slice. If a gauge condition fixes the gauge completely such states cannot exist because they could be added to any physical state while preserving the gauge condition. It may be that the appearance of the extra term indicates that Schnabl gauge has additional subtleties. With a unitary matter CFT, Siegel gauge has no trivial states on the gauge slice. Nor there are such states in Siegel gauge at zero momentum in the standard flat spacetime background. In Schnabl gauge, however, there is a BRST trivial state  $\psi'_0$  that satisfies the gauge condition, making it impossible to fix the gauge completely. The state  $\psi'_0 \sim QB L^+ c_1 |0\rangle$  indeed satisfies the gauge condition:  $BQB L^+ c_1 |0\rangle = LBL^+ c_1 |0\rangle = BLL^+ c_1 |0\rangle = 0$ . It is truly trivial since it is  $Q$  of something which is in the gauge. The state  $\psi'_0$  plays a key role in the tachyon vacuum solution and features in the difficulties to construct exactly marginal solutions for general operators in Schnabl gauge [9].

If we do not use the symmetrized prescription for  $\mathcal{P}$  we cannot even obtain (4.55). We will not attempt here to discuss the possible implications of (4.55) for the computation of string amplitudes, nor if it reflects a shortcoming of the gauge condition or a shortcoming of the presently defined propagator.

To derive (4.55) we begin with

$$\mathcal{P}_{\Lambda\Lambda^*}\mathcal{K} = \frac{B}{L_\Lambda} Q \frac{B^*}{L_{\Lambda^*}} (-C^* B^* QBC) = \frac{B}{L_\Lambda} \frac{L^*}{L_{\Lambda^*}} QBC = \frac{B}{L_\Lambda} (1 - e^{-\Lambda^* L^*}) QBC, \quad (4.56)$$

and rewrite this as

$$\begin{aligned} \mathcal{P}_{\Lambda\Lambda^*}\mathcal{K} &= \frac{B}{L_\Lambda} QBC - \frac{B}{L_\Lambda} Q e^{-\Lambda^* L^*} BC \\ &= \frac{L}{L_\Lambda} BC - \frac{L}{L_\Lambda} e^{-\Lambda^* L^*} BC + QB \frac{1}{L_\Lambda} e^{-\Lambda^* L^*} BC. \end{aligned} \quad (4.57)$$

Expanding the first two terms one gets

$$\mathcal{P}_{\Lambda\Lambda^*}\mathcal{K} = (1 - e^{-\Lambda L} - e^{-\Lambda^*L^*} + e^{-\Lambda L}e^{-\Lambda^*L^*})BC + QB\frac{1}{L_\Lambda}e^{-\Lambda^*L^*}BC. \quad (4.58)$$

Consider the terms inside the parentheses. As  $\Lambda$  becomes large the term  $e^{-\Lambda L}$  will give a singular surface – thus no contribution. The same holds for  $e^{-\Lambda^*L^*}$  for large  $\Lambda^*$ . The last term,  $e^{-\Lambda L}e^{-\Lambda^*L^*}$ , is more delicate. It vanishes in our prescription, since one gets a singular surface as soon as one parameter ( $\Lambda$  or  $\Lambda^*$ ) goes to infinity. Interestingly, if we take  $\Lambda = \Lambda^*$  then  $e^{-\Lambda L}e^{-\Lambda L^*} \sim e^{-L^+}$  and this gives a regular surface. We thus see that, apart from the  $Q$  exact term, we get the expected answer – just  $BC$  – for the symmetrized prescription and not from the prescription (4.28), for example.

Let us now examine the extra  $Q$  trivial term in (4.58). Comparing with (4.55) we identify  $\eta$ :

$$\eta = B\frac{1}{L_\Lambda}e^{-\Lambda^*L^*}BC. \quad (4.59)$$

Clearly  $B\eta = 0$ . Let us now see if  $BQ\eta = 0$ . Using also  $Be^{-\Lambda^*L^*} \simeq -e^{-\Lambda^*L^*}B^*$ , which holds for large  $\Lambda^*$  (see (C.47)), we get

$$BQ\eta = \{B, Q\}\eta = \frac{L}{L_\Lambda}Be^{-\Lambda^*L^*}BC = -(1 - e^{-\Lambda L})e^{-\Lambda^*L^*}B^*BC. \quad (4.60)$$

With the symmetrized prescription the final right-hand side vanishes, as desired. We thus confirm the structure predicted in (4.55). This is evidence that our definition of the propagator is consistent with its fundamental role as an inverse of the kinetic term.

Before concluding this section we discuss another rewriting of the propagator. With the benefit of hindsight we can write the propagator in a form that makes the exchange symmetry more transparent. Instead of commuting  $Q$  to the right as in (4.4), we symmetrize over the two ways of commuting  $Q$ ,

$$\mathcal{P}_{\Lambda\Lambda^*} = \frac{1}{2} \left[ \frac{B}{L_\Lambda} - \frac{B}{L_\Lambda} \frac{B^*}{L_{\Lambda^*}} Q - \frac{B}{L_\Lambda} e^{-\Lambda^*L^*} \right] + \frac{1}{2} \left[ \frac{B^*}{L_{\Lambda^*}} - Q \frac{B}{L_\Lambda} \frac{B^*}{L_{\Lambda^*}} - e^{-\Lambda L} \frac{B^*}{L_{\Lambda^*}} \right]. \quad (4.61)$$

The first group of terms is the result of moving  $Q$  to the right and the second group is the result of moving  $Q$  to the left. There are now two boundary terms, which we can bring to a common form by a few applications of the CBH formula. For the first boundary term,

$$\begin{aligned} \frac{B}{L_\Lambda} e^{-\Lambda^*L^*} &= \int_{\frac{s^*}{s}}^{s^*} \frac{dx}{x} e^{-x(1-\frac{1}{s^*})L^+} e^{[(x-\frac{1}{x})+\frac{1-x}{s^*}]L} \cdot \left[ \frac{1}{s^*}B + \left( \frac{1}{s^*} - 1 \right) B^* \right] \\ &\cong \int_{\frac{s^*}{s}}^{\infty} \frac{dx}{x} e^{-xL^+} e^{(x-\frac{1}{x})L} \cdot (-B^*). \end{aligned} \quad (4.62)$$

In the last line we have dropped terms that are subleading for large  $s = e^\Lambda$  and  $s^* = e^{\Lambda^*}$ , irrespective of how the limits are taken. For the second boundary term,

$$\begin{aligned}
e^{-\Lambda L} \frac{B^*}{L_{\Lambda^*}^*} &= \int_{\frac{1}{s}}^{\frac{s^*}{s}} \frac{dx}{x} e^{-(x-\frac{1}{s})L^+} e^{[(x-\frac{1}{x})+\frac{1}{s}(\frac{1}{x}-1)]L} B^* \\
&\cong \int_0^{\frac{s^*}{s}} \frac{dx}{x} e^{-xL^+} e^{(x-\frac{1}{x})L} \cdot B^* .
\end{aligned}
\tag{4.63}$$

Apart from the integration ranges, the two boundary terms are exactly equal and opposite. According to the prescription (4.7), we are instructed to average each term over the two values  $s^*/s = 0$  and  $s^*/s = \infty$ . If we take  $s^*/s = \infty$  in (4.62) we have a singular expression with  $x \rightarrow \infty$  and, similarly, if we take  $s^*/s = 0$  in (4.63) we have a singular expression with  $x \rightarrow 0$ . When the propagator is inserted in a generic string diagram, these terms correspond to codimension one loci in moduli space (since  $x$  is fixed to a specific value), where the surface degenerates. It seems safe to assume that these terms give a vanishing contribution. The two remaining possibilities correspond to taking  $s^*/s = 0$  in (4.62) and  $s^*/s = \infty$  in (4.63). The range of  $x$  is from 0 to  $\infty$  in both cases and the two terms cancel each other out.

In summary, when the  $Q$  is moved symmetrically to the left and the right the boundary terms cancel and the propagator can be written as

$$\mathcal{P}_{\Lambda\Lambda^*} = \frac{1}{2} \left[ \frac{B}{L_\Lambda} - \frac{B}{L_\Lambda} \frac{B^*}{L_{\Lambda^*}^*} Q + \frac{B^*}{L_{\Lambda^*}^*} - Q \frac{B}{L_\Lambda} \frac{B^*}{L_{\Lambda^*}^*} \right],
\tag{4.64}$$

with the usual understanding that the cutoffs are removed according to (4.7). In fact, when (4.64) is inserted in a tree level four-point amplitude, the  $\Lambda \rightarrow \infty$  and  $\Lambda^* \rightarrow \infty$  limits commute. The precise definition (4.7) may be necessary for more complicated amplitudes.

## 5 Discussion

The key new features of the Schnabl gauge propagator are the presence of the BRST operator  $Q$  and the need for two Schwinger parameters to represent the operators  $1/L$  and  $1/L^*$ . The BRST action on differential forms on moduli space is familiar [33, 6]. Given some degree  $k$  form  $\Omega_{\Psi_1 \dots \Psi_n}$  labeled by external states  $\Psi_i$ , BRST action gives degree  $k$  forms  $\Omega_{\sum_i \Psi_1 \dots Q \Psi_i \dots \Psi_n}$  where  $Q$  acts on the states, and the degree  $k+1$  exterior derivative  $d\Omega_{\Psi_1, \dots, \Psi_n}$ . Since string amplitudes are integrals of differential forms over moduli space, the action of the various  $Q$ 's arising from the various propagators results in two effects:

1. Some  $Q$ 's end up acting on external states and,

2. Some  $Q$ 's set Schwinger parameters to limit values.

For any given string amplitude the diagrams in which  $Q$ 's act on external states vanish on-shell. These diagrams have more Schwinger parameters than those needed to produce the moduli space, one extra parameter for each  $Q$  that acts on an external state. Our example made this clear: the four-point amplitude includes a string diagram (diagram two) with a  $Q$  acting on external states and, in addition to the modular parameter  $\lambda$ , one extra parameter of integration  $u$ .

The second effect of  $Q$  is more subtle. Previously it was thought that the only relevant boundaries arise when Schwinger parameters go to zero, namely, from collapsed propagators. In the four-string amplitude this familiar boundary gave the on-shell amplitude (diagram one). We have found that a boundary at infinite value of the Schwinger parameter – naively a degenerate surface – can also give a regular contribution. In the four-string amplitude it gave a boundary term that vanished on-shell but helped restore the off-shell exchange symmetry. We do not know if boundaries at infinite values of Schwinger parameters can contribute on-shell in general string amplitudes.

We have obtained a symmetrized form (4.64) of the propagator that is written without boundary terms. In a string diagram with various propagators, boundary terms will arise as the  $Q$ 's are moved across  $B/L$ 's or  $B^*/L^*$ 's in order to get them to act on the external states. We have not discussed the rules needed to deal with these boundaries. Thus, work remains to be done to fully understand tree amplitudes. A better understanding of the propagator might arise by further analysis of how it defines an inverse, following the preliminary discussion at the beginning of §4.3.

In Siegel gauge, an open string diagram has a *spine*: the line formed by the set of all string midpoints on all the propagators – on each strip, the line parallel to the boundaries that divides the strip in two equal parts. In Schnabl gauge the string diagrams map all open string midpoints to infinity. In the disk picture, for example, propagators and states are wedges and all string midpoints are at the center of the disk. The spine thus collapses to a point. It appears that this gives interesting complications for open string loop diagrams. In a planar one-loop amplitude the spine is a curve homotopic to the two boundaries of the annulus diagram. If the spine collapses the annulus becomes singular – it produces the closed string degeneration. It is not clear how finite modulus annuli are produced.

It used to be thought that covariant open string field theory is canonically associated with a certain way to decompose the moduli space of Riemann surfaces [34, 35] – through Strebel quadratic differentials and minimal area string diagrams. We now see that in Schnabl gauge (and presumably in any projector gauge) one finds rather new kind of string diagrams. A good

geometrical understanding of these diagrams may have significant implications for closed string field theory and for closed string physics in open string field theory.

## Acknowledgments

We thank Yuji Okawa for useful comments on a draft version of this paper. LR wishes to thank the Galileo Institute for Theoretical Physics (Florence) and Scuola Normale Superiore (Pisa) for their great hospitality and the INFN for partial support during the completion of this work. The work of B.Z. is supported in part by the U.S. DOE grant DE-FC02-94ER40818. The work of L.R. is supported in part by the National Science Foundation Grant No. PHY-0354776 and by the DOE Outstanding Junior Investigator Award. Any opinions, findings, and conclusions or recommendations expressed in this material are those of the authors and do not necessarily reflect the views of the National Science Foundation.

## A Notation and algebraic identities

In this appendix we collect our main definitions and several useful algebraic identities. We refer to [14, 23, 9] for a more detailed exposition of many of these facts.

### A.1 Basic properties

The operators  $L$  and  $B$  are the zero modes of the stress tensor and of the antighost in the conformal frame of the sliver,

$$L \equiv \oint \frac{d\xi}{2\pi i} \frac{f(\xi)}{f'(\xi)} T(\xi), \quad B \equiv \oint \frac{d\xi}{2\pi i} \frac{f(\xi)}{f'(\xi)} b(\xi), \quad f(\xi) \equiv \frac{2}{\pi} \arctan \xi. \quad (\text{A.1})$$

The superscript  $\star$  indicates BPZ conjugation. We define

$$L^\pm = L \pm L^\star, \quad B^\pm = B \pm B^\star. \quad (\text{A.2})$$

Two basic commutation relations are

$$[L, L^+] = L^+, \quad [B, L^+] = B^+. \quad (\text{A.3})$$

The subscripts  $L$  and  $R$  denote the left and the right part of an operator. We have

$$L^+ = L_L^+ + L_R^+, \quad B^+ = B_L^+ + B_R^+. \quad (\text{A.4})$$



From (A.3) we deduce

$$[L, L_L^+] = L^+, \quad [B, L_L^+] = B_L^+. \quad (\text{A.5})$$

The operators  $L - L_L^+$ ,  $L^* - L_L^+$ ,  $B - B_L^+$ , and  $B^* - B_L^+$  are all derivations of the star algebra. This implies a simple action of  $L$ ,  $L^*$ ,  $B$ ,  $B^*$  on products of string fields:

$$L(\phi_1 * \dots * \phi_n) = (L\phi_1) * \dots * \phi_n + \sum_{m=2}^n \phi_1 * \dots * (L - L_L^+) \phi_m * \dots * \phi_n, \quad (\text{A.6})$$

$$L^*(\phi_1 * \dots * \phi_n) = (L^*\phi_1) * \dots * \phi_n + \sum_{m=2}^n \phi_1 * \dots * (L^* - L_L^+) \phi_m * \dots * \phi_n,$$

$$B(\phi_1 * \dots * \phi_n) = (B\phi_1) * \dots * \phi_n + \sum_{m=2}^n (-1)^{\sum_{k=1}^{m-1} \phi_k} \phi_1 * \dots * (B - B_L^+) \phi_m * \dots * \phi_n,$$

$$B^*(\phi_1 * \dots * \phi_n) = (B^*\phi_1) * \dots * \phi_n + \sum_{m=2}^n (-1)^{\sum_{k=1}^{m-1} \phi_k} \phi_1 * \dots * (B^* - B_L^+) \phi_m * \dots * \phi_n.$$

Here and elsewhere, a string field in the exponent of  $-1$  denotes its Grassmann property: it is 0 mod 2 for a Grassmann-even string field and 1 mod 2 for a Grassmann-odd string field. We also have

$$\begin{aligned} e^{-TL}(\phi_1 * \phi_2 * \dots * \phi_n) &= e^{-TL} \phi_1 * e^{-T(L-L_L^+)} \phi_2 * \dots * e^{-T(L-L_L^+)} \phi_n, \\ e^{-TL^*}(\phi_1 * \phi_2 * \dots * \phi_n) &= e^{-TL^*} \phi_1 * e^{-T(L^*-L_L^+)} \phi_2 * \dots * e^{-T(L^*-L_L^+)} \phi_n. \end{aligned} \quad (\text{A.7})$$

## A.2 Reordering formulas

We often need to reorder exponentials of operators. In all cases, the relevant Lie algebra is two-dimensional, with generators  $x$  and  $y$  and commutation relation  $[x, y] = y$ . Algebraic identities are most easily derived by using the explicit (adjoint) representation of  $x$  and  $y$ :

$$x = \begin{pmatrix} 0 & 1 \\ 0 & 1 \end{pmatrix}, \quad y = \begin{pmatrix} -1 & 1 \\ -1 & 1 \end{pmatrix}. \quad (\text{A.8})$$

As two by two matrices,  $x^2 = x$ ,  $xy = y$  and  $yx = y^2 = 0$ . One then verifies that

$$e^{\alpha x + \beta y} = e^{\frac{\beta}{\alpha}(e^\alpha - 1)y} e^{\alpha x}, \quad \text{when } [x, y] = y. \quad (\text{A.9})$$

Recurrent special cases are:

$$e^{-T(L-L_L^+)} = e^{(1-e^{-T})L_L^+} e^{-TL}, \quad x = L, \quad y = L_L^+ \quad (\text{A.10})$$

$$e^{T(L-L_R^+)} = e^{-(e^T-1)L_R^+} e^{TL}, \quad x = L, \quad y = L_R^+. \quad (\text{A.11})$$

Other identities that can be proved by similar methods are:

$$e^{-TL} B_L^+ = e^{-T} B_L^+ e^{-TL}, \quad (\text{A.12})$$

$$e^{-T(L-L_L^+)} B_L^+ = e^{-T} B_L^+ e^{-T(L-L_L^+)}, \quad (\text{A.13})$$

$$e^{-TL^*} B_L^+ = e^T B_L^+ e^{-TL^*}, \quad (\text{A.14})$$

$$e^{-T(L^*-L_L^+)} B_L^+ = e^T B_L^+ e^{-T(L^*-L_L^+)}. \quad (\text{A.15})$$

### A.3 Wedge states

The wedge states  $W_\alpha$ ,  $\alpha \geq 0$ , are surface states defined by their overlap with a generic Fock state  $\phi$ ,

$$\langle W_\alpha, \phi \rangle \equiv \langle f^{-1} \circ \frac{2}{1+\alpha} \circ f \circ \phi(0) \rangle_{UHP} = \langle f \circ \phi(0) \rangle_{\mathcal{W}_\alpha}. \quad (\text{A.16})$$

In the last equality we have used the definition of the surface  $\mathcal{W}_\alpha$ , the semi-infinite cylinder of circumference  $\alpha + 1$ ,

$$\mathcal{W}_\alpha \equiv \{z \mid \text{Im } z \geq 0, z \sim z + \alpha + 1\}. \quad (\text{A.17})$$

We also use the notation  $\mathcal{C}_\ell$  for the semi-infinite cylinder of circumference  $\ell$ ,

$$\mathcal{C}_\ell \equiv \{z \mid \text{Im } z \geq 0, z \sim z + \ell\}. \quad (\text{A.18})$$

Clearly  $\mathcal{W}_\alpha = \mathcal{C}_{\alpha+1}$ . The state  $W_0 \equiv \mathcal{I}$  coincides with the identity of the star algebra; the state  $W_1 = |0\rangle$  coincides with the  $\text{SL}(2)$  vacuum. The wedge states obey the abelian algebra

$$W_\alpha * W_\beta = W_{\alpha+\beta}. \quad (\text{A.19})$$

In the operator formalism, the wedge states can be written as

$$|W_\alpha\rangle = e^{-\frac{\alpha}{2}L^+} |\mathcal{I}\rangle = e^{-\alpha L_L^+} |\mathcal{I}\rangle. \quad (\text{A.20})$$

The derivations  $L_L^+ - L_R^+$  and  $B_L^+ - B_R^+$  annihilate the identity and commute with  $L^+$ , hence they annihilate all wedge states,

$$(L_L^+ - L_R^+)W_\alpha = (B_L^+ - B_R^+)W_\alpha = 0. \quad (\text{A.21})$$

Other important conservation laws are

$$[(\alpha + 1)L + (\alpha - 1)L^*] W_\alpha = [(\alpha + 1)B + (\alpha - 1)B^*] W_\alpha = 0. \quad (\text{A.22})$$

Some identities for the action of antighost operators on wedge states are:

$$BW_\alpha = (1 - \alpha)B_L^+W_\alpha, \quad (\text{A.23})$$

$$(B - B_L^+)W_\alpha = -\alpha B_L^+W_\alpha, \quad (\text{A.24})$$

$$B^*W_\alpha = (1 + \alpha)B_L^+W_\alpha, \quad (\text{A.25})$$

$$(B^* - B_L^+)W_\alpha = \alpha B_L^+W_\alpha. \quad (\text{A.26})$$

Some identities for the action of Virasoro exponentials on wedge states are:

$$e^{-TL}W_\alpha = W_{e^{-T(\alpha-1)+1}}, \quad (\text{A.27})$$

$$e^{-TL^*}W_\alpha = W_{e^{T(\alpha+1)-1}}, \quad (\text{A.28})$$

$$e^{-T(L-L_L^+)}W_\alpha = W_{e^{-T\alpha}}, \quad (\text{A.29})$$

$$e^{-T(L^*-L_L^+)}W_\alpha = W_{e^{T\alpha}}. \quad (\text{A.30})$$

## B Correlators on the cylinder

We collect here some basic formulas for correlators on  $\mathcal{C}_\ell$ , the semi-infinite cylinder of circumference  $\ell$  defined in (A.18). See also [19]. We introduce the notation

$$s_{ij} \equiv \frac{\sin(\gamma r_{ij})}{\gamma}, \quad \gamma \equiv \frac{\pi}{\ell}. \quad (\text{B.31})$$

The basic ghost correlator is

$$\langle c(r_1) c(r_2) c(r_3) \rangle_{\mathcal{C}_\ell} = s_{12} s_{13} s_{23}. \quad (\text{B.32})$$

From this we readily find

$$\langle c(r_1) c(r_2) \partial c(r_3) \rangle_{\mathcal{C}_\ell} = -\frac{s_{12}}{\gamma} \sin(\gamma(r_1 + r_2 - 2r_3)), \quad (\text{B.33})$$

$$\langle c(r_1) \partial c c(r_2) \rangle_{\mathcal{C}_\ell} = s_{12}^2. \quad (\text{B.34})$$

The operator  $(-B_L^+)$  is represented in the CFT language by an insertion of  $\mathcal{B}$  [19] defined by

$$\mathcal{B} = \int_V \frac{dz}{2\pi i} b(z), \quad (\text{B.35})$$

where  $V$  is a vertical line oriented downwards. The operator  $\mathcal{B}$  can be moved across a ghost insertion with the help of the commutation relations

$$\mathcal{B}c(r) = 1 - c(r)\mathcal{B}, \quad \mathcal{B}\partial c c(r) = -\partial c(r) + \partial c c(r)\mathcal{B}. \quad (\text{B.36})$$

A  $\mathcal{B}$  insertion at the beginning of a correlator can be processed as follows [19]:

$$\langle \mathcal{B} \dots \rangle_{C_\ell} = -\frac{1}{\ell} \left\langle \oint \frac{dz}{2\pi i} z b(z) \dots \right\rangle_{C_\ell}, \quad (\text{B.37})$$

where the contour is over the right boundary upwards and the left boundary downwards. Since  $zb(z)$  transforms as a one-form, this contour can be deformed into a sum of small contours, each encircling a puncture with a ghost insertion. Finally, each contour integral is evaluated with the help of the operator product expansion,

$$\oint \frac{dz}{2\pi i} z b(z) c(r) = r, \quad \oint \frac{dz}{2\pi i} z b(z) \partial c(r) = 1, \quad \oint \frac{dz}{2\pi i} z b(z) \partial c c(r) = c(r) - r \partial c(r), \quad (\text{B.38})$$

where in each case the contour is around the puncture at  $z = r$ , counterclockwise. The simplest application of these techniques is to the correlator

$$\langle \mathcal{B} c(r_1) c(r_2) c(r_3) c(r_4) \rangle_{C_\ell} = -\frac{1}{\ell} (r_1 s_{23} s_{24} s_{34} - r_2 s_{13} s_{14} s_{24} + r_3 s_{12} s_{14} s_{24} - r_4 s_{12} s_{13} s_{23}). \quad (\text{B.39})$$

The matter correlator for  $n$  tachyon vertex operators is

$$\left\langle e^{ip_1 \cdot X(r_1)} \dots e^{ip_n \cdot X(r_n)} \right\rangle_{C_\ell} = (2\pi)^D \delta\left(\sum_{i=1}^n p_i\right) \prod_{i < j} |s_{ij}|^{2\alpha' p_i \cdot p_j}. \quad (\text{B.40})$$

For  $n = 4$ , we can write

$$\begin{aligned} \left\langle e^{ip_1 \cdot X(r_1)} \dots e^{ip_4 \cdot X(r_4)} \right\rangle_{C_\ell} &= (2\pi)^D \delta\left(\sum_{i=1}^4 p_i\right) \cdot |s_{12}|^{-\alpha'(p_1^2 + p_2^2 + \mathbf{s})} |s_{13}|^{\alpha'(\mathbf{s} + \mathbf{t} + p_2^2 + p_4^2)} \\ &\quad \cdot |s_{24}|^{\alpha'(\mathbf{s} + \mathbf{t} + p_1^2 + p_3^2)} |s_{23}|^{-\alpha'(\mathbf{t} + p_2^2 + p_3^2)} |s_{14}|^{-\alpha'(\mathbf{t} + p_1^2 + p_4^2)} |s_{34}|^{-\alpha'(p_3^2 + p_4^2 + \mathbf{s})}, \end{aligned} \quad (\text{B.41})$$

where  $\mathbf{s}$ ,  $\mathbf{t}$ ,  $\mathbf{u}$  are the familiar Mandelstam invariants

$$\mathbf{s} = -(p_1 + p_2)^2, \quad \mathbf{t} = -(p_2 + p_3)^2, \quad \mathbf{u} = -(p_1 + p_3)^2, \quad \mathbf{s} + \mathbf{t} + \mathbf{u} = -\sum p_i^2. \quad (\text{B.42})$$

## C Proof of the rearrangement formula

By the CBH formula, we can reorder the exponentials in (3.36) as

$$e^{-T_1 L} e^{-T_2 L^*} = e^{-\tau_2 L^*} e^{-\tau_1 L}, \quad (\text{C.43})$$

where the parameters  $\tau_i$  are appropriate functions of the parameters  $T_i$ . A simple way to do the calculation is to represent  $L$  and  $L^*$  in the adjoint representation, using (A.8) with  $L = x$  and  $L^* = y - x$ . It is convenient to introduce the notation

$$\bar{t}_i \equiv e^{-T_i}, \quad t_i \equiv e^{-\tau_i}, \quad i = 1, 2. \quad (\text{C.44})$$

We find

$$t_i = \frac{\bar{t}_i}{\bar{t}_1 + \bar{t}_2 - \bar{t}_1 \bar{t}_2}. \quad (\text{C.45})$$

The inverse relations are

$$\bar{t}_1 = \frac{t_1 + t_2 - 1}{t_2}, \quad \bar{t}_2 = \frac{t_1 + t_2 - 1}{t_1}. \quad (\text{C.46})$$

By another application of CBH we find

$$B e^{-\tau L^*} = e^{-\tau L^*} (e^{-\tau} B + (e^{-\tau} - 1) B^*), \quad (\text{C.47})$$

and the BPZ conjugate equation

$$e^{-\tau L} B^* = (e^{-\tau} B^* + (e^{-\tau} - 1) B) e^{-\tau L}. \quad (\text{C.48})$$

Back in (3.36),

$$\frac{B B^*}{L L^*} = \int_0^\infty dT_1 dT_2 (1 - t_1 - t_2) e^{-\tau_2 L^*} B^* B e^{-\tau_1 L}. \quad (\text{C.49})$$

The integration measure can be written as

$$dT_1 dT_2 (1 - t_1 - t_2) = \frac{d\bar{t}_1 d\bar{t}_2}{\bar{t}_1 \bar{t}_2} (1 - t_1 - t_2) = -\frac{dt_1 dt_2}{t_1 t_2} = -d\tau_1 d\tau_2. \quad (\text{C.50})$$

Here we have used the Jacobian determinant

$$\det \frac{\partial(\bar{t}_1, \bar{t}_2)}{\partial(t_1, t_2)} = \frac{t_1 + t_2 - 1}{t_1^2 t_2^2} = \frac{\bar{t}_1 \bar{t}_2}{(t_1 t_2)(t_1 + t_2 - 1)}. \quad (\text{C.51})$$

Note that in the new variables the integration region is given by

$$\mathcal{M} \equiv \{\tau_1, \tau_2 \mid \tau_1 \geq 0, \tau_2 \geq 0, e^{-\tau_1} + e^{-\tau_2} \geq 1\}. \quad (\text{C.52})$$

All in all, we find the simple result

$$\frac{B B^*}{L L^*} = - \int_{\mathcal{M}} d\tau_1 d\tau_2 B^* e^{-\tau_2 L^*} B e^{-\tau_1 L}. \quad (\text{C.53})$$

## References

- [1] G. Veneziano, ‘‘Construction of a crossing-symmetric, Regge behaved amplitude for linearly rising trajectories,’’ *Nuovo Cim. A* **57**, 190 (1968).

- [2] M. Kaku and K. Kikkawa, “The Field Theory Of Relativistic Strings, Pt. 1. Trees,” Phys. Rev. D **10**, 1110 (1974); “The Field Theory Of Relativistic Strings. 2. Loops And Pomerons,” Phys. Rev. D **10**, 1823 (1974).
- [3] E. Witten, “Noncommutative Geometry And String Field Theory,” Nucl. Phys. B **268**, 253 (1986).
- [4] H. Sonoda and B. Zwiebach, “Closed string field theory loops with symmetric factorizable quadratic differentials,” Nucl. Phys. B **331**, 592 (1990).
- [5] H. Sonoda and B. Zwiebach, “Covariant closed string field theory cannot be cubic,” Nucl. Phys. B **336**, 185 (1990).
- [6] B. Zwiebach, “Closed string field theory: Quantum action and the B-V master equation,” Nucl. Phys. B **390**, 33 (1993) [arXiv:hep-th/9206084].
- [7] M. Schnabl, “Analytic solution for tachyon condensation in open string field theory,” Adv. Theor. Math. Phys. **10**, 433 (2006) [arXiv:hep-th/0511286].
- [8] M. Schnabl, “Comments on marginal deformations in open string field theory,” arXiv:hep-th/0701248.
- [9] M. Kiermaier, Y. Okawa, L. Rastelli and B. Zwiebach, “Analytic solutions for marginal deformations in open string field theory,” arXiv:hep-th/0701249.
- [10] E. Fuchs and M. Kroyter, “Marginal deformation for the photon in superstring field theory,” arXiv:0706.0717 [hep-th]. E. Fuchs, M. Kroyter and R. Potting, “Marginal deformations in string field theory,” arXiv:0704.2222 [hep-th].
- [11] M. Kiermaier and Y. Okawa, “Exact marginality in open string field theory: a general framework,” arXiv:0707.4472 [hep-th].
- [12] T. Erler, “Marginal Solutions for the Superstring,” arXiv:0704.0930 [hep-th]; Y. Okawa, “Analytic solutions for marginal deformations in open superstring field theory,” arXiv:0704.0936 [hep-th]. Y. Okawa, “Real analytic solutions for marginal deformations in open superstring field theory,” arXiv:0704.3612 [hep-th].
- [13] I. Kishimoto and Y. Michishita, “Comments on Solutions for Nonsingular Currents in Open String Field Theories,” arXiv:0706.0409 [hep-th]. I. Ellwood, “Rolling to the tachyon vacuum in string field theory,” arXiv:0705.0013 [hep-th].

- [14] L. Rastelli and B. Zwiebach, “Tachyon potentials, star products and universality,” JHEP **0109**, 038 (2001) [arXiv:hep-th/0006240].
- [15] L. Rastelli, A. Sen and B. Zwiebach, “Boundary CFT construction of D-branes in vacuum string field theory,” JHEP **0111**, 045 (2001) [arXiv:hep-th/0105168].
- [16] L. Rastelli, A. Sen and B. Zwiebach, “Classical solutions in string field theory around the tachyon vacuum,” Adv. Theor. Math. Phys. **5**, 393 (2002) [arXiv:hep-th/0102112].
- [17] M. Schnabl, “Wedge states in string field theory,” JHEP **0301**, 004 (2003) [arXiv:hep-th/0201095].
- [18] L. Bonora, C. Maccaferri, R. J. Scherer Santos and D. D. Tolla, “Ghost story. I. Wedge states in the oscillator formalism,” arXiv:0706.1025 [hep-th].
- [19] Y. Okawa, “Comments on Schnabl’s analytic solution for tachyon condensation in Witten’s open string field theory,” JHEP **0604**, 055 (2006) [arXiv:hep-th/0603159].
- [20] E. Fuchs and M. Kroyter, “On the validity of the solution of string field theory,” JHEP **0605**, 006 (2006) [arXiv:hep-th/0603195].
- [21] E. Fuchs and M. Kroyter, “Schnabl’s  $L(0)$  operator in the continuous basis,” JHEP **0610**, 067 (2006) [arXiv:hep-th/0605254].
- [22] L. Rastelli and B. Zwiebach, “Solving open string field theory with special projectors,” arXiv:hep-th/0606131.
- [23] Y. Okawa, L. Rastelli and B. Zwiebach, “Analytic solutions for tachyon condensation with general projectors,” arXiv:hep-th/0611110.
- [24] I. Ellwood and M. Schnabl, “Proof of vanishing cohomology at the tachyon vacuum,” JHEP **0702**, 096 (2007) [arXiv:hep-th/0606142].
- [25] T. Erler, “Split string formalism and the closed string vacuum,” JHEP **0705**, 083 (2007) [arXiv:hep-th/0611200]. “Split string formalism and the closed string vacuum. II,” JHEP **0705**, 084 (2007) [arXiv:hep-th/0612050].
- [26] T. Erler, “Tachyon Vacuum in Cubic Superstring Field Theory,” arXiv:0707.4591 [hep-th].
- [27] C. Imbimbo, “The spectrum of open string field theory at the stable tachyonic vacuum,” Nucl. Phys. B **770**, 155 (2007) [arXiv:hep-th/0611343].

- [28] G. Calcagni and G. Nardelli, “Tachyon solutions in boundary and cubic string field theory,” arXiv:0708.0366 [hep-th].
- [29] S. B. Giddings, “The Veneziano Amplitude From Interacting String Field Theory,” Nucl. Phys. B **278**, 242 (1986).
- [30] S. B. Giddings and E. J. Martinec, “Conformal Geometry and String Field Theory,” Nucl. Phys. B **278**, 91 (1986).
- [31] S. Samuel, “Covariant off-shell amplitudes,” Nucl. Phys. B **308**, 285 (1988). V. A. Kostelecky and S. Samuel, “The Static Tachyon Potential in the Open Bosonic String Theory,” Phys. Lett. B **207**, 169 (1988). R. Bluhm and S. Samuel, “The off-shell Koba-Nielsen formula,” Nucl. Phys. B **323**, 337 (1989).
- [32] H. Fuji, S. Nakayama and H. Suzuki, “Open string amplitudes in various gauges,” JHEP **0701**, 011 (2007) [arXiv:hep-th/0609047].
- [33] L. Alvarez-Gaume, C. Gomez, G. W. Moore and C. Vafa, “Strings In The Operator Formalism,” Nucl. Phys. B **303**, 455 (1988).
- [34] S. B. Giddings, E. J. Martinec and E. Witten, “Modular Invariance in String Field Theory,” Phys. Lett. B **176**, 362 (1986).
- [35] B. Zwiebach, “A Proof that Witten’s open string theory gives a single cover of moduli space,” Commun. Math. Phys. **142**, 193 (1991).